Received: 21 July 2021 | Revised: 24 July 2023 | Accepted: 25 July 2023

DOI: 10.1111/jmg.12742

ORIGINAL ARTICLE

Journal of METAMORPHIC GEOLOGY WILEY

Origin of Erzgebirge ultrahigh-pressure garnetite: Formation from a basaltic protolith by serpentinization-assisted metasomatism?

Esther Schmädicke[1] | **Thomas M. Will**[2]

[1]Geozentrum Nordbayern, Universität Erlangen-Nürnberg, Erlangen, Germany

[2]Institute of Geography and Geology, University of Würzburg, Würzburg, Germany

Correspondence
Esther Schmädicke, Geozentrum Nordbayern, Universität Erlangen-Nürnberg, Schlossgarten 5a, D-91054 Erlangen, Germany.
Email: esther.schmaedicke@fau.de

Funding information
Deutsche Forschungsgemeinschaft, Grant/Award Number: Schm1039/9

Handling Editor: Dr. Katy Evans

Abstract

Erzgebirge ultrahigh-pressure (UHP) garnet peridotite includes scarce layers of garnet pyroxenite, nodules of garnetite and, very rarely, of eclogite. Peridotite-hosted eclogite shows the same subalkali-basaltic bulk rock composition, mineral assemblage and peak conditions as gneiss-hosted eclogite present in the same UHP unit. Garnetite has considerably more Mg, moderately enhanced Ca and Fe and significantly lower contents of Na, Ti, P, K and Si than eclogite, whereas Al is very similar. In addition, the compatible trace elements (Ni, Co, Cr, V) are elevated and most incompatible elements (Zr, Hf, Y, Sr, Rb and rare Earth elements [REE]) are depleted in garnetite relative to eclogite. In contrast to other large ion lithophile elements (LILEs), Pb (+121%) and Ba (+83%) are strongly enriched. The REE patterns of garnetite are characterized by depletion of light and heavy REE and a medium REE hump indicative of metasomatism, features being absent in eclogite. An exceptional garnetite sample shows an REE distribution similar to that of eclogite. Garnetite is interpreted to have formed from the same, but metasomatically altered, igneous protolith as eclogite. Except for Ba and Pb, the chemical signature of garnetite is explained best by metasomatic changes of its basaltic protolith caused by serpentinization of the host peridotite. Garnetite is chemically similar to basaltic rodingite/metarodingite. Although rodingite is commonly more enriched in Ca, there are also examples with moderately enhanced Ca matching the composition of Erzgebirge garnetite. Limited Ca metasomatism is attributed to the preservation of Ca in peridotite during hydrous alteration. This can be explained by incomplete serpentinization favouring metastable survival of the original clinopyroxene. In this case, most Ca is retained in peridotite and not available for infiltration and metasomatism of the garnetite protolith. This inescapable consequence is supported by the fact that clinopyroxene is part of the garnet peridotite UHP assemblage, which would not be the case if Ca had been removed from the protolith prior to

high-pressure metamorphism. The enrichment of compatible elements in garnetite is attributed to decomposition of peridotitic olivine (Ni, Co) and spinel (Cr, V) during serpentinization. Enrichment of Ba and Pb contrasts the behaviour of other LILEs and is ascribed to dehydration of the serpentinized peridotite (deserpentinization). This requires two separate stages of metasomatism: (1) intense chemical alteration of the basaltic garnetite precursor, together with serpentinization of peridotite at the ocean floor or during incipient subduction; and (2) prograde metamorphism and dehydration of serpentinite during continued subduction, thereby releasing Pb–Ba-rich fluids that reacted with associated metabasalt. Finally, subduction to >100 km and UHP metamorphism of all lithologies led to formation of garnetite, eclogite and garnet pyroxenite hosted by co-facial garnet peridotite as observed in the Erzgebirge.

KEYWORDS
Erzgebirge, garnetite, rodingitization, serpentinization, UHP metamorphism

1 | INTRODUCTION

Rodingite is known from various tectonic settings, such as seafloor spreading centres, rifted continental margins, greenstone belts, alpine settings and supra-subduction zones (e.g., Evans, 1977; Laborda-López et al., 2018). There is a close spatial relationship between rodingite and serpentinite occurrences and, given the Ca depletion of serpentinized peridotite and Ca enrichment of many rodingite, there is also a close genetic relationship between rodingitization and serpentinization. These ultramafic rocks are volumetrically minor, but they occur in most, if not all, global orogenic belts and, in addition, contain information useful for deciphering the history of such belts (e.g., Evans et al., 2013). Moreover, they can be used to interpret the tectonic setting in which the rocks originally formed and the one in which they were subsequently chemically modified. In this study, we aim to unravel the origin and formation of garnetite in the Variscan Erzgebirge in central Europe, which may represent an ultrahigh-pressure (UHP) equivalent of rodingite, and attempt to unravel the tectonic processes of how garnetite and associated mafic and ultramafic rocks were incorporated into this orogen.

Rodingite is a CaO-rich and SiO_2- and Na_2O-poor rock that forms by serpentinization of ultramafic rocks, which induces metasomatic changes in adjacent rocks ('rodingitization'). The process typically occurs in oceanic basalt and/or gabbro but also affects other rock types if they occur close enough to serpentinizing peridotite. Rodingitization is characterized by substantial decrease of Si and Na along with increase in Ca content (e.g., Austrheim & Prestvik, 2008; Bach & Klein, 2009; Coleman, 1967; B. W. Evans et al., 1979; Laborda-López et al., 2018; O'Hanley et al., 1992). Originally, the term 'rodingite' was only applied to Ca-rich metasomatic rocks (e.g., Coleman, 1967). However, because the composition of metasomatic rocks, which formed by chemical exchange with serpentinizing peridotite, is highly variable, the term has been used more broadly, including also alkali- and silica-depleted types with only minor Ca enrichment (e.g., Coleman, 1967; Frost et al., 2008; Honnorez & Kirst, 1975; Koutsovitis et al., 2013; O'Hanley et al., 1992; Table S1).

Three high-pressure units (Units 1–3), which consist of high-grade felsic gneiss and intercalated lenses of metabasaltic eclogite, are known from the Erzgebirge, Germany. Units 2 and 3 are high-pressure (HP) units in which lenses of quartz eclogite occur. Unit 1 is a UHP unit containing both gneiss-hosted coesite eclogite and isofacial garnet-bearing ultramafic rocks (e.g., Schmädicke et al., 1992), which are unknown from Units 2 and 3. Garnet peridotite is the dominant ultramafic rock type hosting rare pyroxenite layers and nodules of garnetite (Schmädicke & Evans, 1997). Recently, eclogite, associated with garnetite, in peridotite was reported for the first time from the Erzgebirge UHP unit (Schmädicke & Gose, 2020).

The finding of coesite and diamond in the Erzgebirge (Nasdala & Massonne, 2000; Schmädicke, 1991, 1994) led to a number of studies on eclogite and gneiss focusing on the metamorphic evolution (Rötzler et al., 1998; Schmädicke et al., 1992; Schmädicke & Evans, 1997), timing of metamorphism (Schmädicke et al., 1995, 2018; Tichomirowa et al., 2001; Tichomirowa & Köhler, 2013), water in garnet and pyroxene (Gose & Schmädicke, 2018; Schmädicke & Gose, 2017), and bulk rock composition (Massonne & Czambor, 2007; Schmädicke, 1994;

Schmädicke & Will, 2021). In contrast, the ultramafic rocks were subject to only a few studies exploring the metamorphic peak conditions (Schmädicke & Evans, 1997) and water in garnet (Schmädicke & Gose, 2019, 2020). Moreover, only very little is known about the composition and geochemistry of peridotite (Mathé, 1990) and nothing in this context about peridotite-hosted garnetite and associated eclogite.

Thus, this study is designed to close this gap of knowledge by determining the major and trace element composition of peridotite-hosted garnetite and eclogite with the principal aim to characterize their protoliths and to constrain the petrogenesis. In this context, it is important to disclose the genetic relation of peridotite-hosted garnetite and eclogite and to explore whether peridotite- and gneiss-hosted eclogites have a common origin. Based on the high modal amount of garnet, the composition of garnet (Ca rich) and clinopyroxene (Na poor), and the occurrence of prehnite, Schmädicke and Evans (1997) suggested that garnetite may have formed from a rodingite precursor. In addition, due to the recent finding of peridotite-hosted metabasaltic eclogite occurring next to garnetite, the latter was interpreted as metarodingite (Schmädicke & Gose, 2020). This hypothesis will be tested in this study on the basis of bulk rock composition.

Using novel major, minor and trace element data, it should be possible to test the rodingite hypothesis and other possibilities (e.g., a cumulate origin) and to define the nature of the garnetite protolith, which is important to constrain the origin of Erzgebirge garnet peridotite and associated rocks. The ultramafic rocks have been interpreted as slices from the mantle wedge, which were incorporated into the eclogite-bearing host-rock gneiss during subduction (Schmädicke & Evans, 1997). A similar process referred to as 'intrusion model' was also suggested for ultramafic rocks from the Caledonides (Brueckner, 1998). Such a model explains the presence of garnet-bearing ultramafic rocks in Erzgebirge UHP Unit 1 and their absence in Units 2 and 3. Based on the differences in the depth of burial, that is, >100 km for the UHP Unit 1 and 60–80 km for Units 2 and 3, it is conceivable that only Unit 1 was subducted deeply enough to come in contact with the hangingwall mantle wedge (Schmädicke & Evans, 1997). Thus, it is important to find out whether this model can be reconciled with the new data and the inferred garnetite protolith.

2 | REGIONAL BACKGROUND

The Erzgebirge is located at the northern margin of the Bohemian Massif, the easternmost exposure of basement in the European Variscides. The northeast–southwest-trending Erzgebirge consists of an oval, 80 × 40 km large crystalline complex (Figure 1), which is surrounded by greenschist facies and lower grade metasedimentary sequences. The Erzgebirge basement is made up of a monotonous medium-pressure gneiss–migmatite unit, lacking eclogite facies relics, that is overlain by three HP units (Units 1–3; e.g., Klemd & Schmädicke, 1994; Schmädicke, 1994; Schmädicke et al., 1995). The HP units are composed of high-grade quartzofeldspathic gneiss and intercalated, conformal lenses of metabasaltic eclogite (Figure 1). More than a hundred locations of eclogite and retrogressed equivalents are known in the Erzgebirge (various geological maps 1:25,000; Sächsisches Landesamt, 2020).

In contrast to eclogite, garnet-bearing ultramafic rocks are rare in the Erzgebirge and only present in the UHP Unit 1, where they are aligned in an approximately E–W direction at the southern margin of this unit (Figure 1). The dominant ultramafic rock type is variably serpentinized garnet peridotite that occurs as lenses of a few hundred metres up to 1–2 km length within the same type of felsic, granulitic gneiss (Schmädicke & Evans, 1997). Interlayers of garnet pyroxenite (Mathé, 1990; Schmädicke & Evans, 1997) and nodules of garnetite are locally present (Schmädicke & Evans, 1997). The 1–15 cm thick pyroxenite layers are isoclinally folded, whereas garnetite occurs as linearly aligned

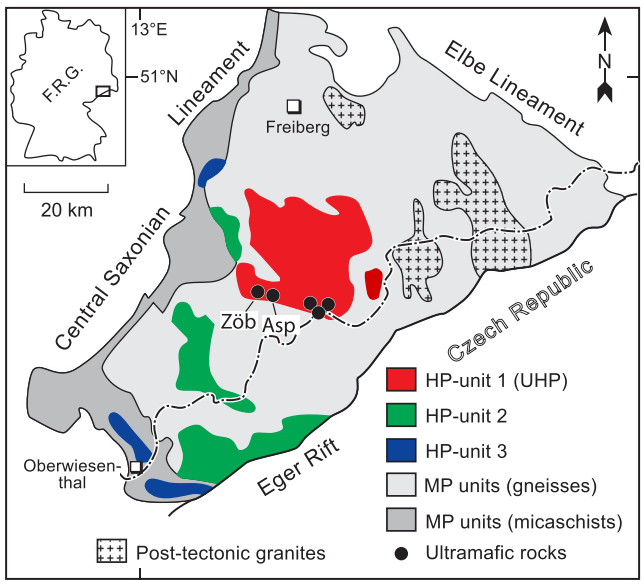

FIGURE 1 Geological map of the Erzgebirge Crystalline Complex modified after Schmädicke et al. (1995) showing the exposure of the three high-pressure (HP) units, the occurrence of ultramafic rocks in the ultrahigh-pressure (UHP) Unit 1 and the sample locations Zöblitz (Zöb) and Ansprung (Asp). MP, medium-pressure.

boudin-like bodies of 10–30 cm length. Garnet peridotite bodies occur in the vicinity of gneiss-hosted UHP eclogite, but the two rock types were not found in direct contact (Schmädicke & Evans, 1997). However, recent field work provided evidence for peridotite-hosted eclogite in an outcrop near Zöblitz (Figure 1; Schmädicke & Gose, 2020). This peridotite-hosted eclogite occurs together with garnetite nodules, which form agglomerates in different parts of the outcrop (Schmädicke & Gose, 2020).

The three HP units differ in their eclogite facies peak conditions, which increase systematically from SW to NE, from Unit 3 (600–650°C, 20–22 kbar), to Unit 2 (670–730°C, 24–26 kbar) and to Unit 1 (840–920°C, ≥30 kbar; Schmädicke, 1994; Schmädicke et al., 1992). Units 2 and 3 contain quartz eclogite, whereas the UHP Unit 1 is characterized by coesite eclogite (Massonne, 2001; Schmädicke, 1991, 1994). Erzgebirge eclogite comprises two colour types: a dominant dark- and a subordinate light-coloured eclogite, both of which occur in all three units (Schmädicke & Will, 2021). The dark type has a homogenous, mid-ocean ridge basalt (MORB)-like basaltic composition, while the chemically variable, Ca–Al-rich and Fe-poor light type was ascribed to plagioclase accumulation in a mid-ocean ridge (MOR) magma chamber (Schmädicke & Will, 2021).

In all three eclogite units, rare HP relics were also found in felsic country rocks, including, for instance, symplectite of sodian diopside and albite (Schmädicke et al., 1992). At one locality in the UHP Unit 1, microdiamond inclusions were found in gneiss (Nasdala & Massonne, 2000; Stöckhert et al., 2001). The presence of diamond, apart from pressure, also points to somewhat higher peak temperature for eclogite from Unit 1 (e.g., ≥870–960°C) if recalculated to 40 kbar, relative to the previous estimate of 840–920°C, which was based on 30 kbar (Schmädicke, 1994; Schmädicke et al., 1992).

Similar metamorphic peak conditions of garnet peridotite and pyroxenite (~900°C, 33–36 kbar) led to the suggestions that they experienced a common metamorphic history together with gneiss-hosted eclogite and the host-rock gneiss (Schmädicke & Evans, 1997). Because all rock types are presumably co-facial, they should have shared a common metamorphic history, at least since the eclogite facies stage of metamorphism. The timing of the latter is defined by Sm–Nd mineral and secondary ion mass spectroscopy (SIMS) U–Pb zircon ages of c. 360 Ma and also constrained by Ar–Ar phengite cooling ages of 348 ± 2 and 355 ± 2 Ma (Schmädicke et al., 1995, 2018). The metabasaltic protoliths are most probably crystallized before c. 540 Ma, as inferred from SIMS U–Pb ages of igneous zircon of eclogite from Units 3 (Schmädicke et al., 2018), 2 and 1 (Tichomirowa & Köhler, 2013).

3 | ANALYTICAL DETAILS

For this study, samples of peridotite-hosted garnetite, eclogite and pyroxenite were investigated petrographically and by geochemical analysis. Thin sections were prepared for each sample used for the geochemical analyses (Table 1) and inspected by a petrographic microscope. For this, rock slices were cut from the hand specimens before crushing and powdering to ensure that the microscopic and geochemical data characterize the same rock volume. Rock powders were generated from the crushed rock pieces by milling in an agate mortar. The sample powders were mixed with a flux (tetraborate), heated to 1000°C in a Pt crucible, and the melt was cast into a Pt mould to generate glass discs. The major element composition of the bulk rocks was obtained on the discs by X-ray fluorescence (XRF) analysis (Table 2) utilizing a Philips PW1480 XRF

TABLE 1 Mineral mode (vol.%) of investigated samples of peridotite-hosted garnetite, eclogite and pyroxenite.

Sample	Locality	Rock type	grt	di	om	qz	rt	op	om-sym	am	zo	Other phases
113a	Zöblitz	Eclogite	40	–	50	3	2	+	+	4[a]	+	op +
113b	Zöblitz	Garnetite	70	28	–	–	2	+	–	–	–	
Zö-Gr	Zöblitz	Garnetite	75	20	–	–	3	–	–	–	–	aggr 2
Zö13-1	Zöblitz	Garnetite	75	24	–	–	1	+	–	–	–	
Zö13-2	Zöblitz	Garnetite	75	23	–	–	1	1	–	–	–	
Zö13-3	Zöblitz	Garnetite	70	29	–	–	1	<1	–	–	–	
Zö13-5	Zöblitz	Garnetite	70	29	–	–	1	+	–	–	–	
32	Ansprung	Pyroxenite	40	48	–	–	+	+	–	+	–	opx 6, aggr 6, ilm <1, phl +

Abbreviations: +, trace; aggr, very fine-grained mineral aggregate; am, amphibole; di, diopside; grt, garnet; ilm, ilmenite; om, omphacite; om-sym, symplectite after omphacite; op, opaque mineral; opx, orthopyroxene; phl, phlogopite; qz, quartz; rt, rutile; zo, zoisite.

[a]Late-eclogitic hornblende with vermicular quartz inclusions.

TABLE 2 Major element composition (wt%) of peridotite-hosted garnetite, eclogite and pyroxenite from Erzgebirge, determined by X-ray fluorescence analysis. For comparison, the average for Unit-1 eclogite was determined from literature data (Schmädicke & Will, 2021).

Sample	113a	113b	Zö-Gr	Zö13-1	Zö-13-2	Zö-13-3	Zö-13-5	32	ecl avg
Rock	Zöb ecl	Zöb gar	Zöb gar	Zöb gar	Zöb gar	Zöb gar	Zöb gar	Asp pyr	Unit 1 ecl
SiO_2	46.0	40.7	38.0	40.5	41.2	41.8	42.9	47.4	48.9
TiO_2	1.5	1.1	1.1	0.6	0.6	0.5	0.9	0.4	1.9
Al_2O_3	16.7	17.6	17.2	17.5	16.8	15.2	14.7	14.6	15.8
Fe_2O_3	12.4	13.9	14.7	14.0	14.2	11.8	13.7	7.7	12.3
MnO	0.22	0.24	0.24	0.24	0.24	0.20	0.22	0.21	0.21
MgO	7.5	12.0	14.5	12.1	12.8	15.5	13.4	19.6	6.6
CaO	12.6	12.8	9.4	12.9	12.2	10.7	11.8	9.0	10.9
Na_2O	2.72	0.28	0.28	0.40	0.54	0.55	0.62	0.52	2.81
K_2O	0.11	0.02	0.05	0.02	0.03	0.25	0.02	0.04	0.14
P_2O_5	0.18	0.11	0.28	0.13	0.15	0.12	0.09	0.11	0.26
LOI	0.00	1.12	4.22	1.58	1.03	3.26	1.29	0.00	0.03
Total	99.84	99.83	99.79	99.85	99.77	99.80	99.75	99.68	99.81

Abbreviations: avg, average; ecl, eclogite; gar, garnetite; pyr, pyroxenite.

spectrometer calibrated against international rock standards. The relative standard deviation was <1% for all elements except for Fe, Mg, Na (<5%) and P (<10%). The trace element data were determined by laser ablation inductively coupled plasma mass spectrometry (LA-ICP-MS; Table 3) at the University of Erlangen-Nuremberg. Using the same glass tablets as for XRF analysis, the concentrations of trace elements were measured with an Agilent 7500c quadrupole LA-ICP-MS, equipped with an UP193FX Excimer laser (New Wave Research). Argon served as plasma, cooling, auxiliary and carrier gas, and He as secondary carrier gas. Spots of 50 μm in diameter were ablated in the melt tablets, applying a repetition rate of 20 Hz and an energy density of 4.35 J/cm^2. Signal integration times for mineral ablation were mostly 25 ms except for Si and Mn (10 ms each) and 20 ms for background. The NIST SRM 612 glass standard (Pearce et al., 1997) was utilized for external calibration, and the SiO_2 concentration determined by XRF analysis for the respective sample served as internal reference. The relative standard deviation (Table S2) is <10% for all elements, except for Tm (12%) and Ta (13%); for 19 elements, the standard deviation is better than 5%. The international geostandard BE-N was prepared and analysed in the same way as the samples and used as secondary standard for testing accuracy (Table S3). Data evaluation was carried out with GLITTER, Version 4.4.4 (van Achterbergh et al., 2000).

4 | RESULTS

4.1 | Petrographic characteristics

The samples of peridotite-hosted garnetite and eclogite were selected from boudin-like nodules of up to 30 cm in diameter occurring within peridotite in a quarry near Zöblitz in the UHP Unit 1 (Figure 1). All garnetite samples (Table 1) come from different nodules. An additional sample of garnet pyroxenite was taken from a 1–15 cm thick interlayer in peridotite that is exposed in a quarry at Ansprung in close vicinity to the Zöblitz locality (Figure 1 and Table 1). Presumably, the rocks exposed in the two outcrops belong to the same ultramafic rocks lens (Mathé, 1990; Schmädicke & Evans, 1997). In contrast to garnetite, peridotite-hosted eclogite is very rare and was only recently described (Schmädicke & Gose, 2020). The studied eclogite sample (113a) was collected from the same nodule as garnetite sample 113b. The following thin section description is focused on the peak metamorphic assemblage and the early post-peak recrystallization under late-eclogitic and amphibolite facies conditions.

4.1.1 | Garnetite

Garnetite is dominated by garnet (70–75 vol.%) and diopsidic clinopyroxene (20–30 vol.%; Table 1 and Figure 2a). Both minerals are chemically homogeneous (Tables S4

TABLE 3 Trace element composition (wt ppm) of peridotite-hosted Erzgebirge eclogite, garnetite and pyroxenite determined by laser ablation inductively coupled plasma mass spectrometry analysis. For comparison, the average for Unit-1 eclogite was determined from literature data (Schmädicke & Will, 2021).

Sample	113a	113b	Zö-Gr	Zö13-1	Zö13-2	Zö13-3	Zö13-5	32	ecl avg
Rock	Zöb ecl	Zöb gar	Zöb gar	Zöb gar	Zöb gar	Zöb gar	Zöb gar	Asp pyr	Unit 1 ecl
Sc	31	58	43	48	51	43	48	40	42
V	324	464	436	474	494	381	428	220	356
Cr	206	161	125	196	189	470	559	1240	208
Mn	1784	1825	2048	2114	2128	1586	1730	1579	1530
Co	43	54	62	49	64	49	60	50	42
Ni	75	82	167	41	141	147	228	512	54
Ge	1.7	1.5	1.4	1.4	1.5	1.3	1.4	1.2	1.4
Rb	6.1	1.1	3.3	1.2	1.5	11	1.4	2,5	4.9
Sr	92	70	19	63	48	53	69	88	117
Y	30	25	19	17	19	8.3	9.4	15	50
Zr	68	49	49	29	29	24	9.4	42	144
Nb	2.6	11	5.7	1.0	1.5	1.4	0.36	0.16	4.6
Mo	0.36	0.54	0.31	0.29	0.35	0.76	0.16	0.50	0.71
Sn	1.2	4.6	3.8	5.2	3.9	1.3	1.0	3.3	2.7
Ba	6.4	14	42	16	133	64	78	13	33
La	3.3	2.8	4.7	1.2	1.4	1.9	1.4	1.9	4.8
Ce	9.9	5.9	15	4.6	5.0	6.5	3.4	4.3	11
Pr	1.5	1.45	2.1	1.0	1.1	1.1	0.43	0.90	2.1
Nd	8.6	11	11	7.7	8.9	7.1	2.4	5.0	12.5
Sm	2.9	6.0	4.7	4.2	4.5	2.8	1.1	1.7	5.0
Eu	1.1	1.3	0.97	1.1	1.0	0.77	0.42	0.55	1.7
Gd	4.2	5.3	3.8	3.5	3.6	2.4	1.4	2.1	7.2
Tb	0.74	0.77	0.57	0.56	0.59	0.33	0.26	0.38	1.3
Dy	5.2	5.0	4.0	3.4	3.8	1.7	1.8	2.7	9.1
Ho	1.1	1.0	0.81	0.72	0.77	0.32	0.41	0.62	2.0
Er	3.3	2.8	2.1	1.9	2.2	0.83	1.0	1.8	5.7
Tm	0.50	0.40	0.32	0.29	0.35	0.11	0.16	0.28	0.84
Yb	3.4	2.4	2.1	1.9	2.1	0.70	1.0	1.8	5.6
Lu	0.49	0.37	0.29	0.25	0.29	0.10	0.15	0.28	0.8
Hf	1.9	1.9	1.6	0.93	0.96	0.76	0.44	1.1	4.1
Ta	0.14	0.92	0.53	0.06	0.09	0.13	0.04	0.06	0.45
W	0.32	1.9	2.4	0.34	0.40	0.63	0.40	0.34	1.6
Pb	1.7	4.3	1.5	5.3	4.5	7.9	3.6	0.73	2.3
Th	0.45	0.75	0.94	0.28	0.27	0.32	0.48	0.27	0.25
U	0.34	0.34	0.93	0.17	0.21	0.21	0.15	0.07	0.38

Abbreviations: avg, average; ecl, eclogite; gar, garnetite; pyr, pyroxenite.

and S5). Rutile and opaque minerals are minor constituents. Quartz is not observed in any sample in contrast to eclogite (Figure 2b). Garnet appears in the form of three textural types: (1) as large grains with up to 5 mm diameter, (2) as recrystallized clusters of small neoblasts (<0.2 mm grain size) replacing some of the large grains

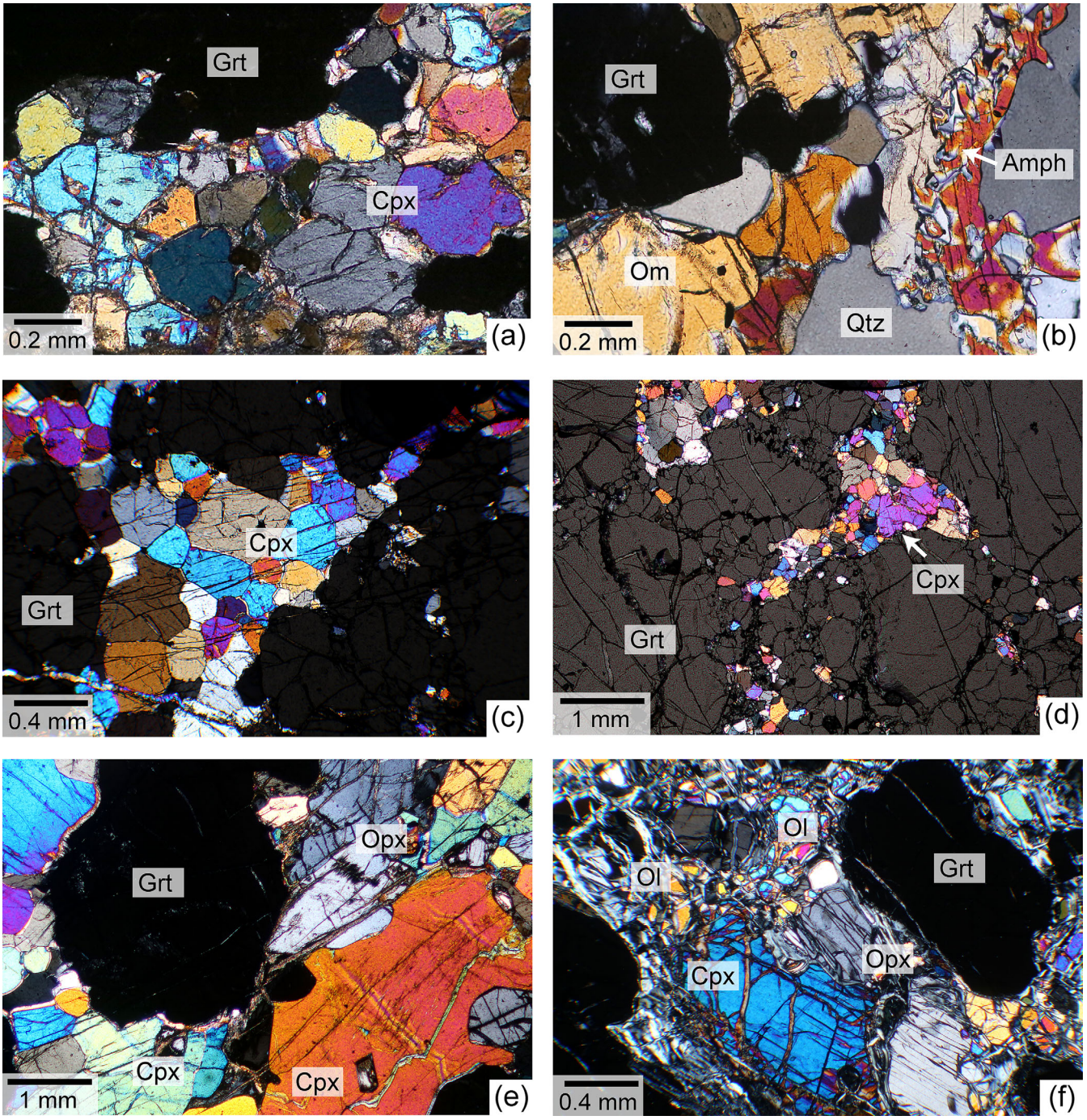

FIGURE 2 Microscopic images of peridotite-hosted garnetite, eclogite and pyroxenite (a–e) and the peridotite host rock (f). Comparison of mineral assemblages and textures of garnetite and eclogite (a, b). (a) Garnet (grt) and diopsidic clinopyroxene (cpx) are the main constituents in garnetite. (b) Apart from garnet and omphacite (om), eclogite contains late-eclogitic calcic amphibole (amph) with inclusions of vermicular quartz. This texture is also common to gneiss-hosted eclogite from the ultrahigh-pressure (UHP) unit and indicates amphibole growth at the expense of omphacite. Quartz (qtz) is a typical constituent of eclogite but it is absent in garnetite. (c, d) Granoblastic texture of garnetite. Clinopyroxene occurs in an interstitial position between larger and partially recrystallized garnet grains. (e) Garnet pyroxenite is dominated by diopsidic clinopyroxene plus garnet and orthopyroxene (opx). (f) The garnet peridotite host rock consists of the metamorphic assemblage garnet, clinopyroxene, orthopyroxene and olivine (ol), which equilibrated at UHP conditions. Retrograde hydrous alteration predominantly affected olivine and led to partial replacement by serpentine. Image (e) was taken with partially crossed polars, and the other images with crossed polars.

and (3) as recrystallized grains within granoblastic garnet–clinopyroxene clusters. Clinopyroxene occurs in such intergrowths together with, or as inclusions in, garnet and monomineralic clusters in interstitial positions between garnet grains (Figure 2c,d). The polygonal granoblastic texture of garnetite together with the lack of visible deformation features indicates that boudinage should have occurred prior to peak metamorphism, most probably during a prograde metamorphic stage at which the rock was already rich in garnet, causing a more rigid (compared with pyroxenite) deformation behaviour.

Retrogressed garnetite is present in some nodules, mostly in association with non-retrogressed portions. The thin section of sample Zö-Gr comprises both primary garnetite (Table 1) and a strongly retrogressed equivalent, which occur as two separate layers. In the retrogressed layer, garnet and clinopyroxene were replaced by very fine-grained, non-identified mineral aggregates. For chemical analysis, only non-retrogressed portions were included.

4.1.2 | Eclogite

The peridotite-hosted eclogite 113a (Table 1) is dark-coloured and macroscopically identical to gneiss-hosted eclogite from Unit 1. Eclogite 113a shows a granoblastic texture devoid of deformation features, similar to that of garnetite. It contains a 'dry' peak assemblage of garnet, omphacite, minor rutile, coesite/quartz and opaque minerals. Example analyses of garnet and omphacite, both having a homogeneous composition, are given in Tables S4 and S5. The average grain size of garnet and omphacite (1–2 mm) is the same as in gneiss-hosted coesite eclogite from Unit 1 but larger than in quartz eclogite from Units 2 and 3 (~0.5 and 0.05–0.1 mm). Garnet also appears as grains as large as 5 mm, similar to associated garnetite. Garnet and omphacite are the major phases with modal proportions of 40 and 50 vol.%, respectively. Post-eclogitic recrystallization is almost absent because symplectite after omphacite is very minor. Calcic amphibole is the only observed hydrous mineral, but it is not part of the peak assemblage. Similar to gneiss-hosted UHP eclogite from Unit 1, calcic amphibole occurs in interstitial positions and invariably contains vermicular inclusions of quartz (Figure 2b). The latter was interpreted as a reaction texture indicative of amphibole growth at the expense of omphacite. This type of amphibole is a distinctive feature of Erzgebirge UHP eclogite as it was never found in the HP units (Gose & Schmädicke, 2018; Schmädicke et al., 1992). Amphibole growth was related to post-peak metamorphic re-equilibration at 25–30 kbar, clearly predating the post-eclogitic symplectite (Schmädicke et al., 1992). Thus, concerning texture and mineral assemblages, peridotite-hosted eclogite is indistinguishable from gneiss-hosted UHP eclogite.

4.1.3 | Garnet pyroxenite

Pyroxenite has a granoblastic texture with clinopyroxene, orthopyroxene and garnet that form an equilibrium assemblage (Figure 2e). The rock is coarse-grained with grain sizes of grt > cpx > opx. About 50% of clinopyroxene grains show exsolution lamellae (up to 3 μm width), which were identified as orthopyroxene (Schmädicke & Evans, 1997). Rutile is a common accessory mineral, which is locally rimmed by ilmenite. Calcic amphibole (up to 1 mm in length) is a rare but characteristic phase. As in eclogite, amphibole occurs in interstitial positions indicative of relatively late growth. Based on the low-energy grain boundaries, amphibole equilibrated with the major minerals. Late formation is also likely for phlogopite.

4.2 | Major and trace element composition

4.2.1 | General characteristics

The composition of peridotite-hosted eclogite (Tables 2 and 3) is indistinguishable from that of the recently studied dark type of gneiss-hosted eclogite from the same unit and also similar to eclogite from Units 2 and 3 (Schmädicke & Will, 2021). All have a subalkali-basaltic composition (Figure 3) that is similar to that of modern MORB (Schmädicke & Will, 2021).

The elemental concentrations of garnetite (Tables 2 and 3) differ from those of associated eclogite although both plot in the field of subalkali basalt (Figure 3). In particular, garnetite has distinctly lower SiO_2 (38.0–42.9 wt%) and Na_2O (0.3–0.6 wt%) concentrations (Figure 4) than eclogite from the same unit (average: 46.0 and 2.7 wt%). In addition, garnetite also has lower TiO_2 (0.5–1.1 vs. 1.5 wt%; Figure 4), Zr, Y (Figure 5) and Hf contents than Unit 1 eclogite (Tables 2 and 3). In contrast, garnetite is strongly enriched in MgO compared with eclogite (12.0–15.5 vs. 7.5 wt%) and consequently has higher Mg# (Mg/[Mg + Fe]: 0.63–0.72, eclogite: 0.55). In addition, compared with the associated eclogite, most garnetite samples have higher concentrations of V, Pb, Ni (Figure 5) and Co (Tables 2 and 3). The pyroxenite sample has much higher Mg# (0.83) and Ni (512 ppm) contents than any sample of eclogite or garnetite (Mg#: 0.47–0.72, Ni: 23–228 ppm; Figure 5).

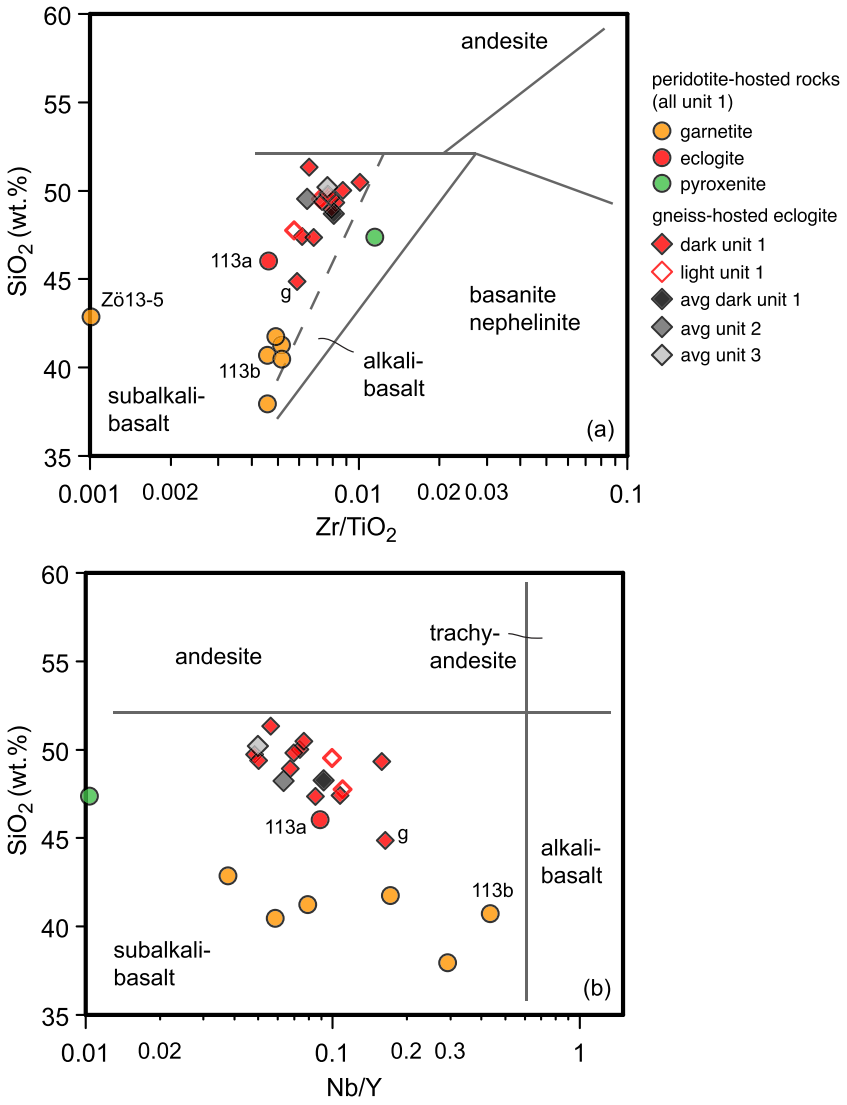

FIGURE 3 Plots of (a) SiO_2–Zr/TiO_2 and (b) SiO_2–Nb/Y after Winchester and Floyd (1977) for investigated samples of peridotite-hosted garnetite, eclogite and pyroxenite. The composition of gneiss-hosted eclogite from Unit 1 and the averages of gneiss-hosted eclogite from all three units, based on data in Schmädicke and Will (2021), are also shown.

Titanium, Zr and Y in garnetite and both peridotite- and gneiss-hosted eclogites from the UHP Unit 1 (but not pyroxenite) are negatively correlated to Mg# (Figures 4 and 5) and MgO (not shown). Additional correlations of Mg# with Al_2O_3, Fe_2O_3, Na_2O, K_2O, Rb, Sr, V, Cr and heavy (H) rare Earth elements (REE) were reported for gneiss-hosted eclogite from Units 1–3 (Schmädicke & Will, 2021). Using the literature data for gneiss-hosted eclogite and including the present data for garnetite, the previously observed correlations are absent or very weak for this extended sample set (Figures 4 and 5). Considering only garnetite, SiO_2 is positively correlated with Na_2O ($r = +0.85$) and negatively with P_2O_5 ($r = -0.90$), Zr ($r = -0.82$) and the light (L)REE from La to Nd ($r = -0.79$ to -0.94).

4.2.2 | REE and trace element patterns

The REE data of peridotite-hosted eclogite define a flat, primitive-mantle normalized pattern (Figure 6a), which corresponds to the REE curves of common (dark-coloured) gneiss-hosted eclogite (Schmädicke & Will, 2021). Comparing the average composition of dark gneiss-hosted eclogite (calculated from data in Schmädicke & Will, 2021) with that of peridotite-hosted eclogite, subtle differences are discernable (Figure 6a). The former has somewhat higher REE concentrations, a weak depletion of LREE and a slight negative Eu anomaly (Figure 6a). However, these average features do not apply to each individual sample (Schmädicke & Will, 2021) that contribute to the average curve of Unit 1 eclogite as shown in Figure 6a. The pyroxenite REE curve exactly parallels that of gneiss-hosted eclogite, but pyroxenite has distinctly lower REE contents (Figure 6a and Table 3).

The REE patterns of garnetite show some variability, with contents of 1–10 times higher than primitive mantle (Figure 6a). One garnetite sample (Zö13-5) is characterized by a pattern that is akin to that of eclogite; only the REE contents are lower. The other garnetite samples show distinct REE fractionation with a pronounced

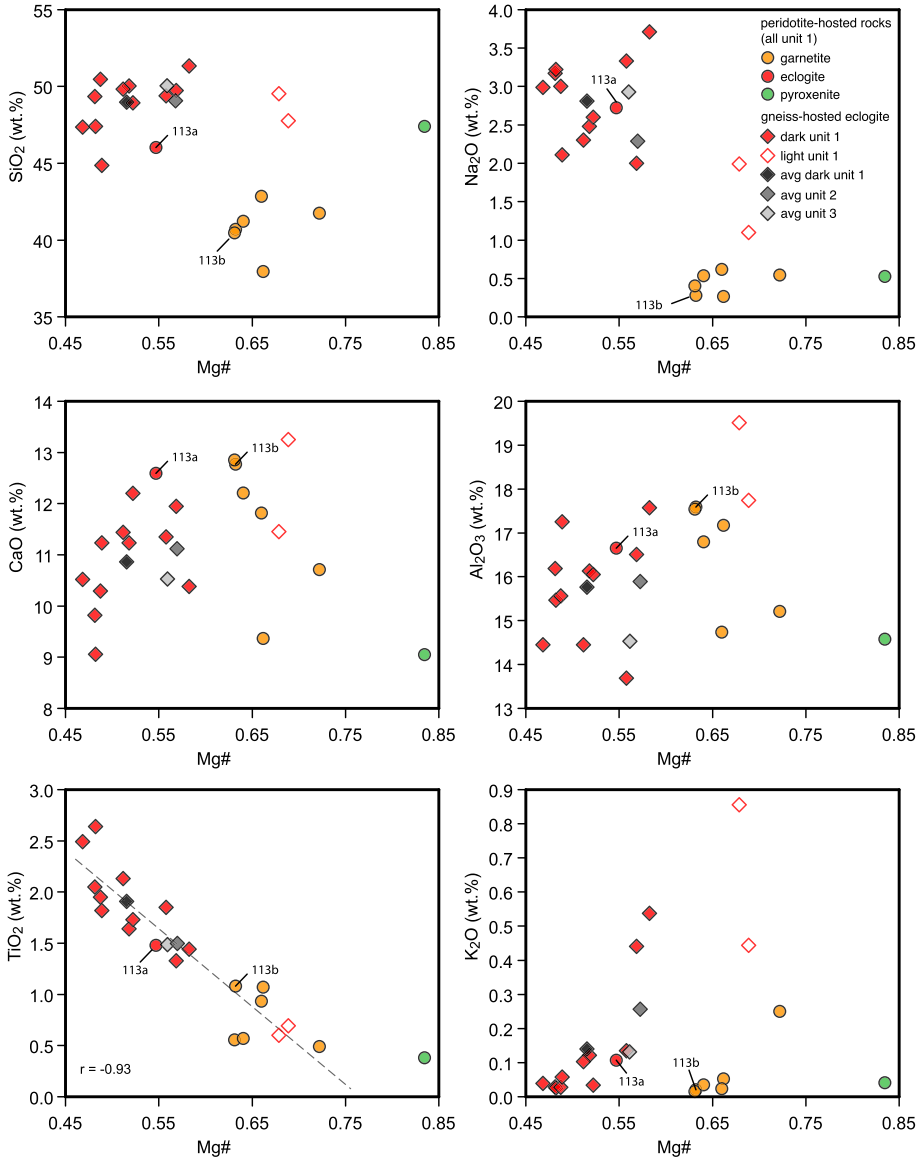

FIGURE 4 Plot of Mg# (MgO/[MgO + FeO]; molar basis) versus SiO_2, Na_2O, CaO, Al_2O_3, TiO_2 and K_2O for investigated samples of peridotite-hosted garnetite, eclogite and pyroxenite. The composition of gneiss-hosted eclogite from Unit 1 (Schmädicke & Will, 2021) and the averages of gneiss-hosted eclogite from all three units are shown for comparison. In the case of elemental correlations, the coefficient *r* is given.

medium (M)REE hump caused by elevated Sm and Nd relative to La, Ce and HREE. The same type of pattern was obtained for garnet from garnetite samples Zö-Gr and Zö13-3 (Schmädicke & Gose, 2020). The LREE and HREE contents in garnetite are lower and the MREE contents are higher than in the associated peridotite-hosted eclogite. Compared with gneiss-hosted eclogite, all REE in garnetite are lower, except of one sample with somewhat higher MREE (Figure 6a).

The primitive-mantle normalized trace element curves of garnetite (Figure 6b) are variable in appearance. They have positive Pb, U and Sm spikes (in decreasing order of magnitude) and negative ones for Sr and Zr. Apart from sample 113b, they also have negative Nb peaks. The peridotite-hosted eclogite (113a) shares the positive peaks for Pb and U, but not for Sm, and the negative one for Sr, but not for Zr. Part of the garnetite samples shows a positive Ba spike, whereas peridotite-hosted eclogite (113a) and gneiss-hosted eclogite exhibit a negative Ba peak (Figure 6b). The element pattern of pyroxenite reveals a strong negative Nb spike but is otherwise rather smooth compared with the other rock types.

5 | DISCUSSION AND CONCLUSIONS

5.1 | Possible protoliths

The geochemical data indicate that peridotite-hosted eclogite has a subalkali-basaltic (or gabbroic) precursor that is indistinguishable from that of common (dark), gneiss-hosted Erzgebirge eclogite (Schmädicke &

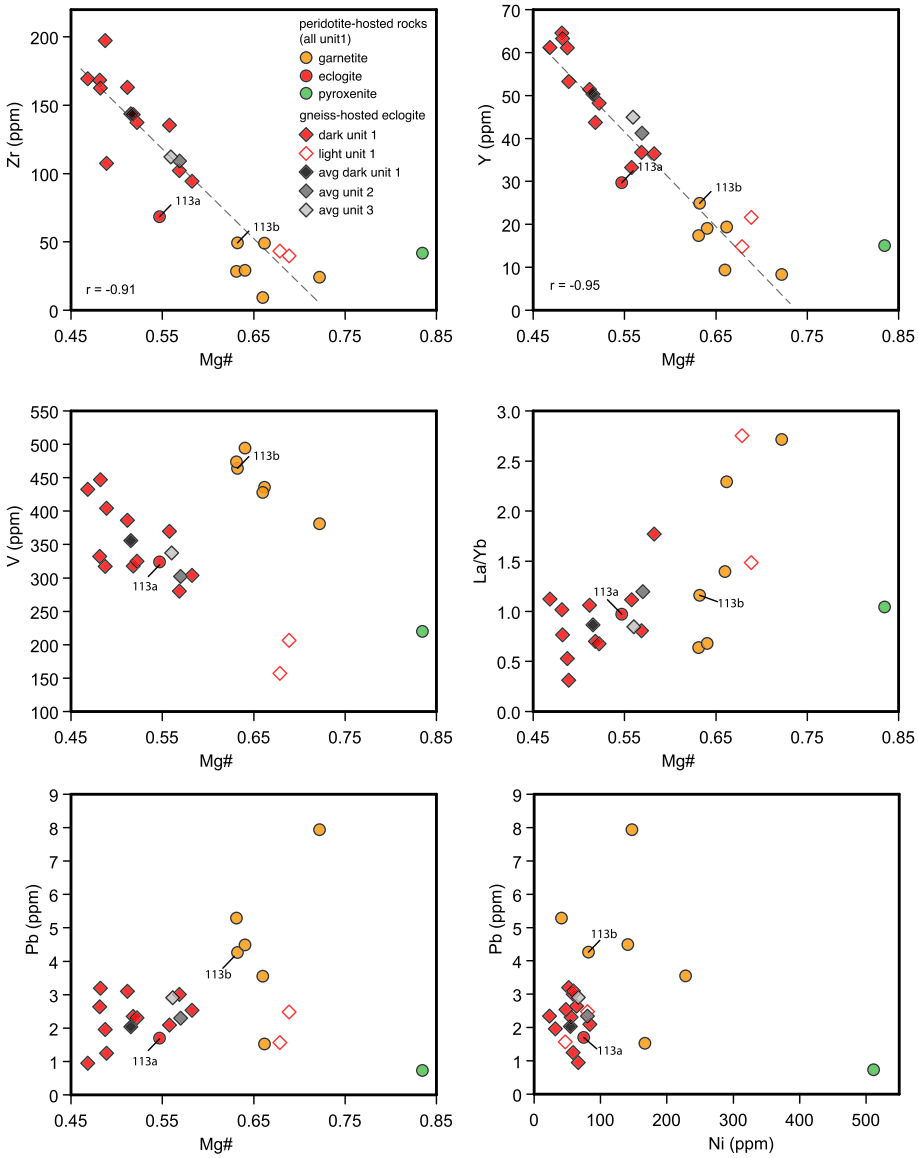

FIGURE 5 Plot of Mg# (MgO/[MgO + FeO]; molar basis) versus Zr, Y, V, La/Yb, Pb and of Ni versus Pb for investigated samples of peridotite-hosted garnetite, eclogite and pyroxenite. The composition of gneiss-hosted eclogite from Unit 1 (Schmädicke & Will, 2021) and the averages of gneiss-hosted eclogite from all three units are shown for comparison. In the case of elemental correlations, the coefficient *r* is given.

Will, 2021), which occurs in the same unit. Garnetite has a near-basaltic composition but, compared with both, the common dark and the very rare light, types of Erzgebirge eclogite, it has unusually low SiO_2 and Na_2O and relatively high MgO, Ni and Co contents. Other components in garnetite, such as TiO_2, Zr, Hf, Y and REE, are lower than in dark eclogite but overlap with concentrations of the rare and chemically more variable light eclogite type, which was interpreted in terms of plagioclase accumulation in an MOR magma chamber (Schmädicke & Will, 2021). Vanadium contents, on the other hand, are considerably higher in garnetite than in light eclogite. Garnet pyroxenite has a composition similar to that of many worldwide pyroxenite examples (see compilation in Schmädicke, Will, & Mezger, 2015) that occur in orogenic settings and formed by interaction of mafic melts with mantle rocks.

Concerning the igneous precursor of garnetite, a clinopyroxene cumulate or a picritic protolith could be envisaged given the high Mg content. However, the Al and Ca contents of garnetite do not agree with the former and that of Fe not with the latter possibility (Schmädicke, Will, & Mezger, 2015). Instead, the chemical signature of garnetite can well be reconciled with a basaltic precursor, similar to that of eclogite, that was chemically modified by metasomatic alteration. A common (basaltic) protolith for both rock types is supported by the fact that peridotite-hosted eclogite and garnetite exclusively occur in close spatial relation and never separately. Further possibilities are that garnetite formed from a metasomatically altered pyroxenite precursor or may represent the metamorphic equivalent of an olivine–plagioclase cumulate, both of which being consistent with high Mg, Ni and Co contents.

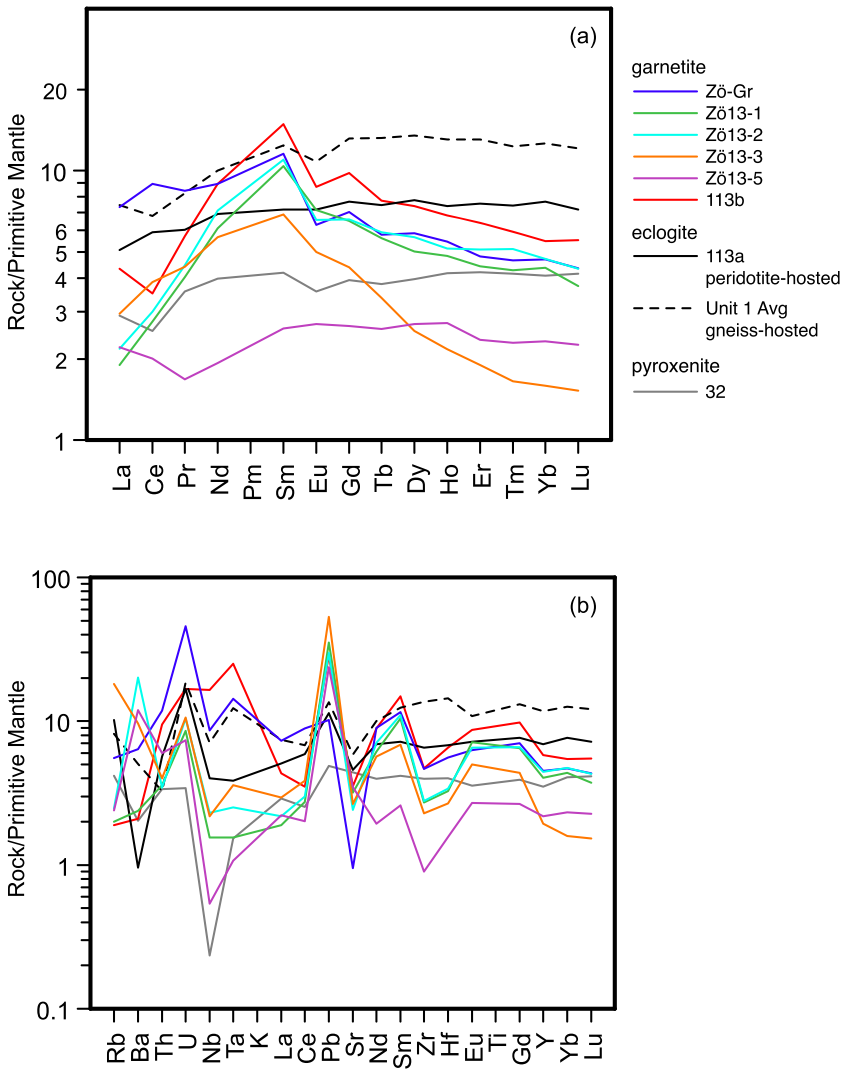

FIGURE 6 Rare Earth element (a) and trace element (b) patterns for investigated samples of peridotite-hosted garnetite, eclogite and pyroxenite. The average composition of the common (dark) gneiss-hosted eclogite from Unit 1 (using data from Schmädicke & Will, 2021) is also shown. Values are normalized to primitive mantle (McDonough & Sun, 1995).

Of the three remaining possibilities, an olivine–plagioclase cumulate (or troctolite) is the least likely protolith of garnetite. First, this is because garnetite, like dark eclogite, has a distinct negative Sr spike and no or a slightly negative Eu anomaly (Figure 6). This is in marked contrast to the positive Eu and Sr spikes indicative of plagioclase accumulation and typical for cumulative troctolite and gabbro (e.g., Berno et al., 2019; Coogan et al., 2002). Second, the calculated hypothetical bulk rock compositions for variable mixtures of olivine and plagioclase, using Mg# and Na/Ca of garnetite as a measure for mineral composition (Table S6), do not match the composition of garnetite and clearly contradict a cumulate origin. Adding clinopyroxene to the calculations even increases the mismatch (Appendix S1 and Table S7).

Thus, it seems unlikely that garnetite formed from an unaltered igneous protolith. The possibility that garnetite originated from a metasomatically altered precursor rock can be evaluated with the aid of Gresens-type plots (Gresens, 1967; Figure 7). As suggested above, garnetite may well have formed by metasomatism from the same basaltic protolith as eclogite (hereafter also named 'eclogite protolith'). In addition, metasomatically altered pyroxenite is also an option.

Starting with the latter possibility and assuming constant volume, a pyroxenite protolith for garnetite would require severe loss of Mg and Si plus gain of Fe, Ca, Al and Ti (Figure 7a). Another option is to use Al as a reference frame because it is considered as the least mobile major element in metamorphic processes (Grant, 2005), but this leads to the same result. However, the occurrence of garnetite in peridotite and its absence in any other rock type implies that metasomatism was genetically related to the host peridotite in which case metasomatic exchange should lead to the opposite trend for Mg (gain) and Ti (loss). In addition, the nodular shape of garnetite bodies can hardly be reconciled with the morphology of pyroxenite occurring as layers in peridotite. For these reasons, a pyroxenite precursor for garnetite is very unlikely.

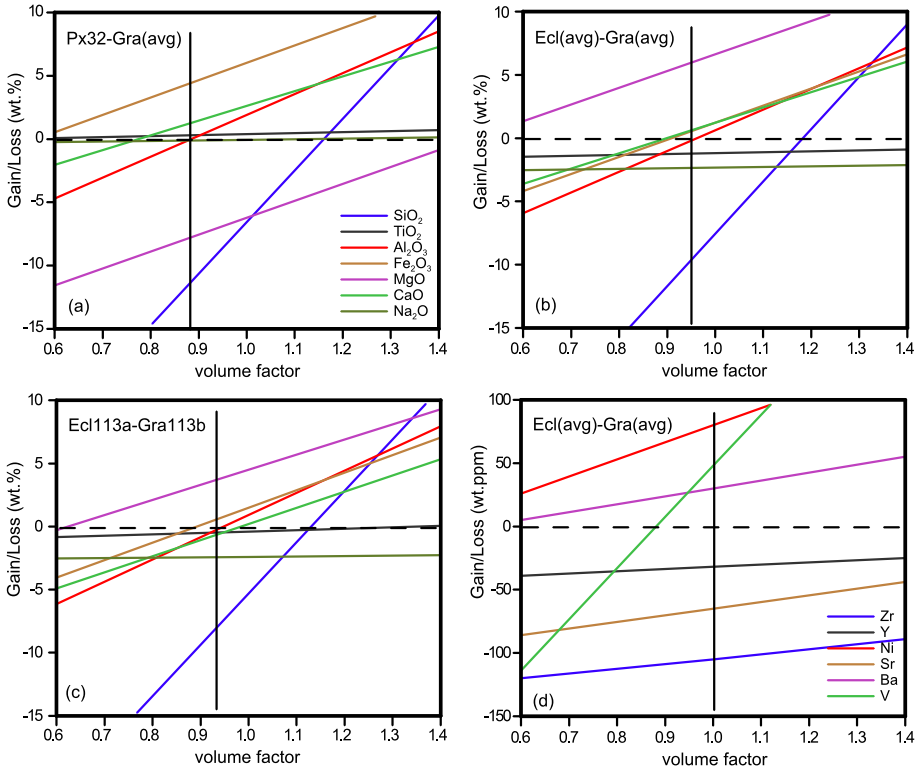

FIGURE 7 Gresens-type plots (Gresens, 1967) for major (a–c) and selected trace elements (d). (a) Pyroxenite 32 and garnetite (average). (b, d) Eclogite (average) and garnetite (average). (c) Eclogite 113a and garnetite 113b. Garnetite (metarodingite) presumably formed from the same protolith as eclogite due to addition of Mg and removal of Si, Na and Ti (b, c). Using an Al reference frame indicates a volume factor of ~0.95 signifying moderate volume loss. The changes in trace elements (d) are compatible with metasomatic exchange between the basaltic eclogite protolith and peridotite/serpentinite, except of Ba enrichment (see text for explanation). Assuming a pyroxenite precursor for garnetite (c) requires Mg loss, which cannot be reconciled with exchange reactions with peridotite/serpentinite.

A different picture arises if garnetite formed from the metasomatically altered basaltic protolith of eclogite. Based on the average bulk rock composition and constant volume, an origin of garnetite from such a precursor would have involved considerable loss of Na and Ti and a strong gain of Mg as well as moderate removal of Si and addition of Ca, Fe and minor Al (Figure 7b). Using Al as a reference frame, a minor volume loss of ~5% (volume factor = 0.95; Figure 7b) is indicated but element loss or gain is basically the same as with constant volume. Apart from using average eclogite and garnetite composition, another possibility is to compare the eclogite and garnetite samples 113a and 113b (Figure 7c), which occur in the same nodule, with each other. The result for these two rocks (Figure 7c) is very similar to that obtained for average bulk rock compositions (Figure 7b) even though it cannot be excluded that eclogite 113a itself—given by the small size of the nodule—experienced some degree of metasomatic exchange with the surrounding peridotite. The occurrence of both rock types in one nodule implies differential access to the metasomatizing fluid.

Thus, a metasomatized basaltic protolith of garnetite can be reconciled with (i) the higher mobility of Si, Na and Mg compared with Fe, Ca and Al and (ii) the modifications expected due to chemical exchange with a Mg-rich and Na-, Si- and Ti-poor peridotitic host rock. In addition, the MREE hump shown by most garnetite samples (but not by eclogite) is also a characteristic feature of metasomatism (e.g., Burgess & Harte, 2004; Smith & Griffin, 2005). Notably, a single garnetite sample reveals an REE pattern similar to eclogite. Taken together, it is very likely that garnetite and eclogite formed from the same magmatic precursor and, accordingly, that garnetite represents the metasomatically altered equivalent of eclogite. Pursuing this option and including minor and trace elements in Gresens- (Figure 7d) and Grant-type plots (Grant, 2005) implies that metasomatism involved loss of K and P (Figure 8a) as well as of Zr, Y, Sr, Rb and REE (Figure 8b), as expected for chemical exchange of a basaltic protolith with peridotite. The same applies to the observed gain of Ni, Co, Cr and V (Figure 8b). Only the addition of Ba and Pb to the protolith of garnetite is difficult to explain in this context (see last section).

Compared with the average composition of eclogite, the most pronounced relative element increase in garnetite (i.e., >50 wt%) is observed for Ni (+134%), Pb (+121%), Mg (+101%), Ba (+83%) and Cr (+52%; Table 4). Elements affected by the greatest loss are Na (−83%), Zr (−80%), Hf (−76%), Ti (−62%), P (−54%), K (−51%), Sr (−48%), LREE (−56%) and HREE (−65 to −71%). The relative changes for major elements, apart from Mg, are more moderate and amount to a 15% loss of Si, an 11% gain for Ca, a 10% increase for Fe and Mn, and a 4% increase for Al (Table 4). These values apply to constant volume, which appears to be reasonable given that very little change in Al content (~0.5 wt%) would be involved in this case. Thus, the volume of garnetite is

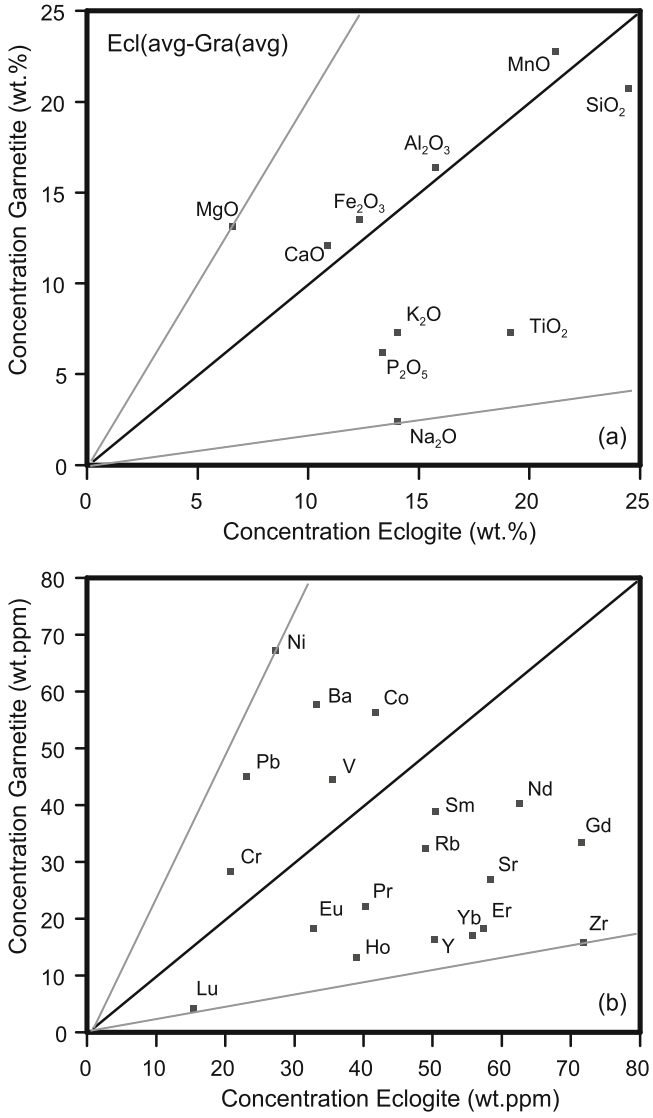

FIGURE 8 Isocon diagrams ('Grant-type' plots; Grant, 2005) for major (a) and trace elements (b) using the average composition of garnetite (metarodingite) and eclogite from Unit 1. Elements above/below the black solid line were added to/removed from garnetite relative to eclogite. The plots visualize the greatest gain for Mg (+101%; grey line in (a)), Ni (+134%; grey line in (b)), Pb (+121%) and Ba (+83%) and the greatest loss for Na (−83%; grey line in (a)) and Zr (−80%; grey line in (b)).

estimated to be in the range of 95 (using Al as a reference frame) to 100% relative to the eclogite protolith.

We infer (1) that garnetite is the HP equivalent of metasomatically altered basalt or gabbro and (2) that the associated UHP eclogite formed from the same, but unaltered, basaltic protolith. Particularly, the occurrence of a nodule containing both garnetite (113b) and eclogite (113a) is a strong argument for a common magmatic precursor of both rock types. The finding that only peridotite-hosted—but not gneiss-hosted—basaltic protoliths were chemically modified is a further, clear indication that metasomatism of the garnetite protolith must be related to interaction with its host peridotite; otherwise, garnetite should occur elsewhere in the Erzgebirge given the more than hundred occurrences of gneiss-hosted eclogite (or its retrogressed equivalents).

5.2 | Metasomatism of a basaltic protolith in a peridotite host

Metasomatism of basalt/gabbro due to interaction with ultramafic rocks is known from numerous worldwide examples of such rock associations (see below). The elemental changes in the mafic rocks are designated as 'rodingitization' and attributed to serpentinization of associated peridotite (e.g., Austrheim & Prestvik, 2008; Bach & Klein, 2009; Coleman, 1967; B. W. Evans et al., 1979; Laborda-López et al., 2018; O'Hanley et al., 1992). Rodingized rocks are characterized by significantly lower Si and Na and higher Ca contents compared with the unaltered protoliths. Indeed, the studied Erzgebirge garnetite has a significantly lower Na_2O content (−83% relative) and also lower SiO_2 (−15%) and higher CaO (+11%) contents than eclogite with an unaltered basaltic composition (Table 4). Although many literature examples of rodingite are characterized by a stronger increase in CaO (e.g., B. W. Evans et al., 1979; Koller & Richter, 1984; Laborda-López et al., 2018), the compositional data for rodingite or metarodingite, respectively, are extremely variable and include examples with relatively low CaO content, even lower compared with Erzgebirge garnetite (see Table S1). For instance, CaO contents of 9.6–13.8 wt%, being similar to those of the inferred (or exposed) basaltic protoliths, were reported for metarodingite from various occurrences (Coleman, 1967; Koutsovitis et al., 2013; Li et al., 2008; O'Hanley et al., 1992; Salvioli-Mariani et al., 2020) and also for non-metamorphic rodingite from the Mid-Atlantic Ridge with CaO contents as low as 10.5 wt% (Honnorez & Kirst, 1975). In addition, garnetite xenoliths (95–100 vol.% garnet) interpreted as metarodingite contain 8.1–12.9% CaO (Smith & Griffin, 2005; Table S1). These concentrations match those of the Erzgebirge garnetite (9.4–12.8% CaO) very closely and imply that rodingitization of a basaltic protolith can occur without severe Ca metasomatism.

Similar to Ca, the overall changes of other major elements reported in the literature and related to rodingitization of basaltic rocks are extremely variable. For instance, Al behaves usually as immobile during the process (e.g., Duan et al., 2021; Grant, 2005; Koutsovitis et al., 2013), but there are also examples of increasing

TABLE 4 Major (wt%) and selected trace element (wt ppm) composition of Erzgebirge garnetite compared with gneiss-hosted dark eclogite from Unit 1. The average for Unit-1 eclogite was determined from literature data (Schmädicke & Will, 2021); the average of garnetite excludes sample Zö-Gr.

	ecl avg Unit 1	gar avg	gar–ecl absolute	gar–ecl %		ecl avg Unit 1	gar avg	gar–ecl absolute	gar–ecl %
SiO_2	48.97	41.40	−7.6	−15	Rb	4.9	3.2	−1.7	−34
TiO_2	1.91	0.73	−1.2	−62	Sr	116.8	60.8	−56.0	−48
Al_2O_3	15.76	16.38	0.6	4	Y	50.3	15.8	−34.5	−69
Fe_2O_3	12.31	13.52	1.2	10	Zr	143.7	28.2	−115.5	−80
MnO	0.21	0.23	0.0	10	Ba	33.2	60.9	27.7	83
MgO	6.55	13.16	6.6	101	Ce	11.4	5.1	−6.3	−56
CaO	10.86	12.07	1.2	11	Pr	2.1	1.0	−1.1	−51
Na_2O	2.81	0.48	−2.3	−83	Nd	12.5	7.4	−5.1	−41
K_2O	0.14	0.07	−0.1	−51	Sm	5.0	3.7	−1.3	−26
P_2O_5	0.26	0.12	−0.1	−54	Eu	1.7	0.9	−0.7	−44
LOI	0.03	1.66			Gd	7.2	3.3	−3.9	−55
Total	99.81	99.80			Dy	9.1	3.1	−6.0	−65
					Er	5.7	1.8	−4.0	−69
Co	41.8	55.1	13.3	32	Yb	5.6	1.6	−3.9	−71
Ni	54.5	127.8	73.3	134	Lu	0.8	0.2	−0.6	−71
V	356.0	448.1	92.1	26	Hf	4.1	1.0	−3.1	−76
Cr	207.7	314.9	107.1	52	Pb	2.3	5.1	2.8	121

Abbreviations: avg, average; ecl, eclogite; gar, garnetite.

and decreasing Al contents during rodingitization (e.g., Austrheim & Prestvik, 2008; B. W. Evans et al., 1979; Gussone et al., 2020; Honnorez & Kirst, 1975; Schandl et al., 1989). Magnesium and Fe contents can also be variable although, more typically, Mg tends to be enriched in most cases (Coleman, 1967; Honnorez & Kirst, 1975; O'Hanley et al., 1992; Palandri & Reed, 2004) and Fe remains more or less unchanged during rodingitization of basalt/gabbro (e.g., Koutsovitis et al., 2013; O'Hanley et al., 1992). This closely agrees with our results of Erzgebirge garnetite, characterized by enhanced Mg and constant Fe concentrations relative to the basaltic precursor. The diversity of elemental behaviour during rodingitization was ascribed to variations in parameters such as temperature, pressure, oxygen fugacity, alkalinity and CO_2 content of the fluid, the fluid–rock ratio and closed or open system behaviour (e.g., Bach & Klein, 2009; Duan et al., 2021; Koutsovitis et al., 2013; Laborda-López et al., 2018; O'Hanley et al., 1992; Palandri & Reed, 2004). In addition, rodingite from one occurrence can be mineralogically and chemically inhomogeneous and element enrichment or depletion may vary across a single body (e.g., Austrheim & Prestvik, 2008; Laborda-López et al., 2018; Li et al., 2008) testifying to disequilibrium on outcrop scale.

Further information on protolith origin is provided by the trace element characteristics of Erzgebirge garnetite (low in Ti, Zr, Y, REE and large ion lithophile element [LILE]; high in Ni, Co, Cr and V) compared with literature data from similar, metasomatized rocks. For example, removal of Ti, Zr and LILEs was described also for rodingitized basaltic rocks from the Zermatt-Saas ophiolite (Li et al., 2008). Depletion of Ti, Y, Zr and REE was also found in rodingite from Greece and explained by the action of a highly alkaline fluid (Koutsovitis et al., 2013). High alkalinity was attributed to low-temperature serpentinization (e.g., Frost & Beard, 2007) and depletion of REE to high fluid–rock ratios (e.g., Bau, 1991; Gillis et al., 1992). The data for Erzgebirge garnetite, compared with those of eclogite (Schmädicke & Will, 2021), also signify removal of LREE and HREE but preservation of MREE (Figure 6). In addition, enhanced contents of compatible trace elements (Ni, Co, Cr, V) and of Mg, as in the Erzgebirge samples, are also known from other locations (e.g., Koutsovitis et al., 2013; Li et al., 2008).

In conclusion, literature data imply that removal of Si and Na (and other alkali elements) seems to be a hallmark of rodingitization (Bach & Klein, 2009; Frost et al., 2008) while the addition of Ca is very common, but not ubiquitous, and its extent can strongly vary in a

single body. Removal of Si and Na from the basaltic precursor of rodingite was attributed to seafloor alteration of plagioclase in a low silica-activity environment (Frost et al., 2008). This may well also apply to Erzgebirge garnetite and explain the low, as well as the mutually correlated, contents of Si and Na. The observed depletion of LREE and HREE can be ascribed to the decomposition of igneous clinopyroxene, being the main REE carrier in the basaltic protolith, and providing for REE mobilization during hydration and metasomatic exchange with the serpentinizing fluid. Retention of MREE causes a hump-shaped REE pattern, similar to those observed in xenoliths from the cratonic mantle (whole rocks and garnet) and ascribed to metasomatism (e.g., Schmädicke, Gose, et al., 2015; Smith & Griffin, 2005; Stachel et al., 2004). In the present case, the hump may point to replacement of clinopyroxene by calcic amphibole, which has a strong preference for MREE (e.g., Botazzi et al., 1999). Enrichment of Mg, Ni and Co in the basaltic protolith during metasomatism is attributed to the breakdown of olivine, and the increase of Cr and V may be related to decomposition of spinel in the peridotite host rock.

We conclude that the specific composition of Erzgebirge garnetite resulted from metasomatism, similar to rodingitization, of a basaltic/gabbroic protolith driven by metasomatic exchange with the peridotite host during serpentinization—as previously inferred on the basis of mineral composition (Schmädicke & Evans, 1997; Schmädicke & Gose, 2020).

5.3 | Rodingitization with little or no Ca metasomatism?

Rodingitization of basaltic rocks is commonly linked with Ca enrichment so that the term 'rodingite' originally was applied to Ca-rich metasomatic rocks (e.g., Coleman, 1967). However, because metasomatic rocks that formed during serpentinization of adjacent peridotite have a highly variable composition, the term has been used more broadly including alkali- and silica-depleted rock types with only slightly enhanced or even non-elevated Ca content (e.g., Coleman, 1967; Frost et al., 2008; Honnorez & Kirst, 1975; Koutsovitis et al., 2013; O'Hanley et al., 1992; Table S1). Erzgebirge garnetite seems to be a further example of moderate Ca enrichment (~11%). So why is the Ca content of metasomatized basaltic rocks, modified during serpentinization, so different? Based on literature data, we discuss and evaluate possibilities that may be responsible for the chemical variability.

Calcium metasomatism has been attributed to release of Ca from peridotite during serpentinization (e.g., Austrheim & Prestvik, 2008). In turn, the lack of Ca metasomatism was ascribed to the preservation of Ca in decomposing peridotite (Frost et al., 2008) and the latter authors concluded that the removal of Si from basaltic rocks is a universal feature of rodingitization but Ca metasomatism is not, and may or may not occur. But, again, what is the reason for this?

In this context, the source of Ca is important. One possible donator is seawater, and the other is decomposing peridotite. Though peridotite is low in Ca, during hydration of peridotite, the element is released to the serpentinizing fluid from decomposing clinopyroxene (e.g., Iyer et al., 2008; Miyashiro et al., 1969). A local, peridotite source of Ca was also inferred from several other studies that imply that Ca is mantle derived (Austrheim & Prestvik, 2008; Bach & Klein, 2009; Gussone et al., 2020). Direct evidence is provided by Ca isotope data that clearly signify a mantle signature (Gussone et al., 2020). The results of the present study imply that Erzgebirge garnetite formed most likely from a basaltic precursor due to metasomatic exchange with the host peridotite during serpentinization. Given that Ca was locally provided by decomposing ultramafic rocks, we still need to explain why CaO was only moderately (11% relative) enriched in the garnetite protolith. One option is that pronounced Ca metasomatism actually did occur in the first place but was followed by secondary depletion, a process referred to as 'de-rodingitization' (e.g., Koutsovitis et al., 2013; O'Hanley et al., 1992). The second possibility is a high fluid–rock ratio during metasomatism in which case compositional gradients are diminished (Bach & Klein, 2009). However, a high fluid–rock ratio is unlikely in the present case because the elemental budget of the metasomatizing fluid would not be buffered by serpentinization, which, however, is a necessary prerequisite to explain the elemental signature of garnetite such as high Mg, Ni, Co, Cr and V contents and low concentrations of Si, Na, K, Ti, P and of most incompatible trace elements.

A third reason might be the preservation of peridotitic clinopyroxene during serpentinization. This, in fact, is the most likely explanation for the Erzgebirge rocks and, possibly, also for other examples of metasomatized basaltic rocks with non-modified to moderately elevated Ca content. If clinopyroxene did not decompose during hydrous alteration, Ca could not have been released from peridotite and added to the basaltic precursor of garnetite. This line of reasoning is strongly supported by the fact that clinopyroxene is a ubiquitous constituent of the HP assemblage of Erzgebirge peridotite (Schmädicke & Evans, 1997; Figure 2f), which would be impossible if Ca had already been removed from its protolith during serpentinization. The invariable presence of

clinopyroxene in the host garnet peridotite, together with limited Ca enrichment in the enclosed garnetite nodules, is a strong argument for a linkage between Ca metasomatism and clinopyroxene pointing to a local, peridotitic Ca source.

Notably, clinopyroxene (or a large part of it) is observed to survive as a metastable phase in partially serpentinized ultramafic rocks and is not hydrated until olivine and orthopyroxene are completely replaced (e.g., Dungan, 1979). Data from abyssal peridotite show a pronounced negative correlation ($r = -0.87$) between the bulk rock CaO content and the degree of serpentinization (Table S8 and Figure S1). In other words, if serpentinization runs to completion and equilibrium is attained (i.e., clinopyroxene decomposed entirely), a great part of Ca is mobilized and only negligible amounts of it remain in serpentinite. In turn, peridotite, being partially serpentinized, may still contain a disproportionally large amount of CaO bound to metastable clinopyroxene. In the case of insufficient (or completely lacking) mobilization of Ca in peridotite, metasomatism and Ca enrichment in adjacent mafic rocks are limited.

Because clinopyroxene has a greater resistance to serpentinization than olivine and orthopyroxene (e.g., Mével, 2003), clinopyroxene (and CaO) is apt to metastable preservation in partially serpentinized peridotite. This was shown in experiments (Marcaillou et al., 2011) and reported from many natural samples (e.g., Dungan, 1979; Iyer et al., 2008; Seyler et al., 2003). In abyssal peridotite with reaction extent of 60–90%, olivine was completely replaced by serpentine whereas clinopyroxene and spinel were retained (Seyler et al., 2003). In contrast, completely serpentinized peridotite consists of serpentine minerals + magnetite ± talc ± brucite ± tremolite ± chlorite without any relics of clinopyroxene (e.g., Bach et al., 2004; K. A. Evans & Frost, 2021; Mével, 2003; Miyashiro et al., 1969; Palandri & Reed, 2004). Incomplete serpentinization could be due to restricted fluid supply. This is expected in a sub-seafloor or mantle-wedge setting where fluid pathways may become sealed by volume expansion as serpentinization of peridotite progresses. It is also possible that sluggish reaction rates due to low and/or progressively decreasing temperature contributed to incomplete serpentinization of peridotite. Whatever the reason for partial serpentinization, the presence of clinopyroxene in the well-equilibrated UHP assemblage of Erzgebirge peridotite and the relatively high CaO bulk rock contents (range: 1.3–2.8 wt%; Mathé, 1990) provide evidence for the preservation of Ca due to metastable survival of most clinopyroxene of the original ocean-floor or mantle-wedge peridotite.

5.4 | Implications for protolith origin of Erzgebirge garnetite

This study implies that the subalkali-basaltic precursor of Erzgebirge eclogite, both gneiss and peridotite hosted, was also the protolith of garnetite. However, in the latter case, the original basalt/gabbro was affected by metasomatic alteration. It was shown that the protolith gneiss-hosted Erzgebirge eclogite originated at an oceanic spreading centre (Schmädicke & Will, 2021), which, by implication, also applies to the igneous precursor of garnetite. Such an ocean-floor origin was also inferred for many other eclogites in the Bohemian Massif and spatially related complexes (Beard et al., 1995; Koglin et al., 2018; Stosch & Lugmair, 1990; Timmermann et al., 2004; Will et al., 2015; Will & Schmädicke, 2001; Woodland et al., 2002). However, the occurrence of garnetite (or similar rocks of metasomatic origin) is a unique feature of the Erzgebirge, unknown from any other Variscan eclogite unit where such rocks may occur but have not been described yet.

Serpentinization of peridotite and chemical modification of the associated basaltic protolith of garnetite are possible in different tectonic settings. First, metasomatism could have taken place during ocean-floor metamorphism close to a spreading centre as suggested for several rodingite occurrences (e.g., Austrheim & Prestvik, 2008; Bach & Klein, 2009; Frost et al., 2008; Honnorez & Kirst, 1975). In the context of this model (model a; Figure 9), Erzgebirge garnet peridotite must have formed from a low-pressure, oceanic crustal precursor rock. If correct, the Erzgebirge ultramafic rocks cannot have been incorporated into the subducting eclogite-bearing units as exotic UHP slices of garnet peridotite derived from the hangingwall mantle as proposed by Schmädicke and Evans (1997). Second (model b; Figure 9), metasomatism of basalt/gabbro and serpentinization of peridotite occurred during subduction of oceanic crust (e.g., Coleman, 1967; Koutsovitis et al., 2013; Li et al., 2008) and were facilitated by the formation of bending faults that provided fluid pathways at brittle conditions (e.g., Ranero et al., 2003). Concomitant subduction of the protoliths of garnetite, eclogite and garnet peridotite, again, implies an abyssal, ocean-floor precursor for all rock types. Other possibilities such as metasomatism (rodingitization) during exhumation (Li et al., 2007) and/or chemical modification due to fluid–rock interaction during return flow within or along a subduction channel (e.g., Deschamps et al., 2013) are excluded in the present case, because the bulk rock chemical modification of the Erzgebirge rocks clearly pre-dates UHP metamorphism.

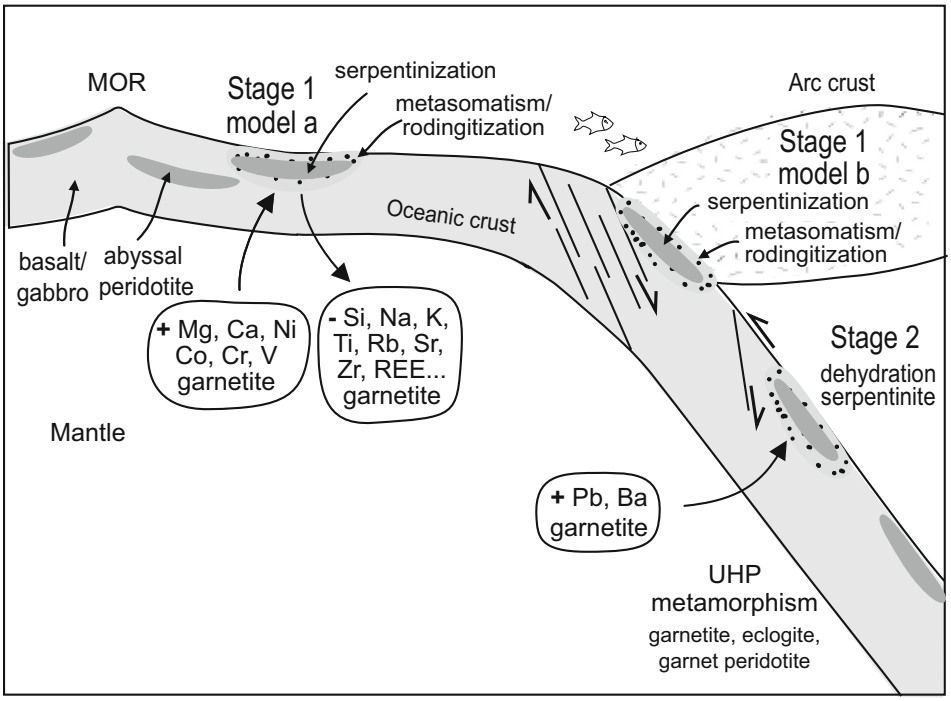

FIGURE 9 Schematic sketch model showing the two metasomatic stages. (1) Serpentinization of abyssal peridotite and contemporaneous metasomatism (rodingitization?) of gabbro or basalt was governed by brittle faulting and fluid influx, either in the vicinity of a spreading centre (model a) or at moderate depth in a subduction zone (model b). (2) Subduction to greater depths led to dehydration of serpentinite and release of Pb–B-rich fluid, which was added to the metasomatized gabbro/basalt. Finally, the rock association underwent ultrahigh-pressure (UHP) metamorphism resulting in formation of garnetite (metarodingite?) and garnet peridotite. MOR, mid-ocean ridge; REE, rare Earth elements.

Metasomatism of the basaltic garnetite precursor mainly involved gain of Mg (101% increase), Ca (11%), Fe (10%) plus compatible trace elements (Ni, Cr, Co, V) and removal of Na, Ti, P, K and Si (decreasing order) and of most incompatible trace elements such as Zr, Hf, Y, Sr, Rb and REE, but not of Ba and Pb. These results demonstrate that Erzgebirge garnetite shares significant characteristics with many other rodingite/metarodingite examples on a global scale. However, there are also features that are unique to the Erzgebirge samples, particularly the strongly enhanced Pb (121%) and Ba (83%) contents, while the other LILEs are reduced. Metasomatism, including rodingitization, may lead to elevated and reduced LILE contents within a single outcrop (Austrheim & Prestvik, 2008). However, the decoupling of Pb and Ba from other LILEs does not conform with a simple single-stage metasomatic process leading to either depletion or enrichment of LILEs. The marked enrichment of Pb and Ba can only be explained by two discrete metasomatic events. The first of which is related to ocean-floor processes (see above), and the second to the early stages of prograde metamorphism as outlined below.

Serpentinite is known to contain relatively high amounts of Pb and Ba (Deschamps et al., 2013; Hattori & Guillot, 2003; Pettke & Bretscher, 2022; Schwarzenbach et al., 2018; Tenthorey & Hermann, 1979). In addition, experiments, simulating serpentinite breakdown in subduction zones, showed that the fluid/residue partition coefficient is very high for these elements (i.e., 30–250; Tenthorey & Hermann, 1979). Thus, fluid released from dehydrating serpentinite should be Pb and Ba rich. Accordingly, the enrichment of the two elements in Erzgebirge garnetite is attributed to dehydration of associated serpentine-bearing peridotite (or serpentinite) during the early stages of prograde metamorphism, liberating Pb- and Ba-rich fluid. Apart from fluid-mobile elements, deserpentinization is considered to be isochemical (e.g., K. A. Evans & Frost, 2021) so that this process is unlikely to modify the major element content of serpentinite and, in turn, of adjacent rocks.

We conclude that metasomatism of the basaltic protolith of Erzgebirge garnetite can best be explained by two independent stages of element transfer, each of which involving a different type of fluid. The first stage (stage 1; Figure 9) was related to serpentinization of associated peridotite at relatively low temperature and pressure conditions, either close to an oceanic ridge (model a) or at shallow depth in a subduction zone (model b; Figure 9). The liberated fluid that equilibrated with the hydrating peridotite reacted with the basaltic garnetite protolith where it caused chemical changes that are similar to those described for rodingite (gain of Mg, Ca and Fe, compatible trace elements; removal of Na, Ti, Si and K, incompatible trace elements). During further subduction and prograde metamorphism (stage 2; Figure 9), serpentinite dehydrated and released a Ba- and Pb-enriched fluid that refertilized the metasomatically altered and LILE-depleted basaltic garnetite protolith at intermediate depths. Subsequently, continued subduction of both the mafic (garnetite and eclogite) and ultramafic rocks (garnet peridotite) to at least 100 km depth led to UHP

metamorphism at relatively high temperature giving rise to the well-equilibrated UHP assemblages in garnetite (garnet and diopside), eclogite (omphacite, garnet and coesite) and peridotite (garnet, diopside, enstatite and olivine; Schmädicke, 1991; Schmädicke et al., 1992; Schmädicke & Evans, 1997). The fact that diopside is a common constituent of the UHP assemblage of garnet peridotite invariably indicates that only minor amounts of Ca could have been removed from the abyssal peridotite precursor during low-temperature alteration. This was probably due to incomplete serpentinization that led to metastable survival of clinopyroxene. This, in turn, explains why Ca metasomatism in associated basaltic protolith of garnetite was moderate compared with many (but not all) reported examples of rodingite/metarodingite.

5.5 | General implications

Our findings provide new petrogenetic insights with respect to (i) ocean-floor and subduction-zone metamorphism and metasomatism of mafic and ultramafic rocks and (ii) the tectonic incorporation of mantle rocks into the continental crust that have implications well beyond the Erzgebirge and the Variscan orogen. We speculate that rocks with chemical features similar to those of the garnetite described in this study cannot be unique to the Erzgebirge but must also be present in other orogens given the widespread occurrence of hydrated ocean-floor basalt/gabbro and associated serpentinite and the fact that at least some examples share many chemical characteristics with Erzgebirge garnetite (e.g., Honnorez & Kirst, 1975; Table S1), except for Pb and Ba. The latter contrast, however, is easily explained. Enrichment of Pb and Ba in basalt/gabbro is governed by deserpentinization of adjacent ultramafic rocks, which takes place due to increasing temperature in a subduction-zone setting. Hence, ocean-floor basalt/gabbro that has not been subducted yet but was solely altered by ocean-floor metamorphism should have the same (or lower) Pb and Ba contents as its unaltered precursor. However, as soon as hydrated and partially metasomatized mafic and ultramafic ocean-floor rocks become entrained in a subduction zone, they start to dehydrate. Release of Pb and Ba from decomposing serpentine provides for enrichment of these elements in the associated mafic rocks, which, given their widespread occurrence, should be a common feature. Maybe such 'doubly metasomatized' mafic rocks exposed in orogenic belts are more difficult to recognize if they were not subducted deep enough to form HP/UHP assemblages and/or if they are strongly retrogressed, but they should occur in more locations than presently known.

A related question is how mantle-derived garnet peridotite became incorporated into the continental crust. Such orogenic (or alpine-type) peridotites are volumetrically minor components in HP and UHP terranes that formed by continental subduction and collision but are known from many locations worldwide (e.g., Liou et al., 1998, 2007), including the Variscan Erzgebirge (Schmädicke & Evans, 1997). It was suggested that garnet peridotite was directly incorporated into deeply subducted crust (>60 km) from the hangingwall lithospheric mantle by tectonic erosion (e.g., Brueckner, 1998; Schmädicke & Evans, 1997) or from the asthenospheric mantle due to slab break-off (Schmädicke et al., 2010). Alternatively, garnet peridotite may form from a low-pressure precursor, such as ocean-floor peridotite or serpentinite, by deep subduction and HP/UHP metamorphism (e.g., Evans & Trommsdorff, 1978). In the latter case, incorporation of the ultramafic rocks in the continental crust could have occurred during any stage of subduction or exhumation. It is also conceivable that ultramafic, mafic and felsic lithologies were already in contact prior to subduction or were juxtaposed during incipient subduction, as in a passive continental margin setting. Because, in the Erzgebirge UHP unit, the different lithologies shared a common metamorphic evolution from the UHP peak stage onwards (Schmädicke & Evans, 1997), we can conclude that they came in contact either prior to or during subduction. This agrees with the results of the present study, which imply hydrated, low-temperature precursor rocks for garnetite, eclogite and peridotite.

ACKNOWLEDGEMENTS

The authors are indebted to Kathy Evans (Perth) for kindly overtaking the editorial handling and her helpful and constructive suggestions. Four anonymous reviewers are thanked for their critical comments. We thank Helene Brätz and Melanie Hertel (Erlangen) for their help with the ICP and XRF analysis. This work was supported by Deutsche Forschungsgemeinschaft (DFG grant Schm1039/9). Open Access funding enabled and organized by Projekt DEAL.

ORCID

Esther Schmädicke https://orcid.org/0000-0002-0522-8210

REFERENCES

Austrheim, H., & Prestvik, T. (2008). Rodingitization and hydration of the oceanic lithosphere as developed in the Leka ophiolite, north-central Norway. *Lithos*, *104*, 177–198. https://doi.org/10.1016/j.lithos.2007.12.006

Bach, W., Garrido, C. J., Paulick, H., Harvey, J., & Rosner, M. (2004). Seawater–peridotite interactions: First insights from ODP Leg 209, MAR 15°N. *Geochemistry, Geophysics, Geosystems*, *5*, Q09F26. https://doi.org/10.1029/2004GC000744

Bach, W., & Klein, F. (2009). The petrology of seafloor rodingites: Insights from geochemical reaction path modeling. *Lithos*, *112*, 103–117. https://doi.org/10.1016/j.lithos.2008.10.022

Bau, M. (1991). Rare-earth element mobility during hydrothermal and metamorphic fluid–rock interaction and the significance of the oxidation state of europium. *Chemical Geology*, *93*, 219–230. https://doi.org/10.1016/0009-2541(91)90115-8

Beard, B. L., Medaris, L. G. Jr., Johnson, C. M., Jelínek, E., Tonika, J., & Riciputi, L. R. (1995). Geochronology and geochemistry of eclogites from the Mariánské Lázně Complex, Czech Republic: Implications for Variscan orogenesis. *Geologische Rundschau*, *84*, 552–567. https://doi.org/10.1007/BF00284520

Berno, D., Sanfilippo, A., Zanetti, A., & Tribuzio, R. (2019). Reactive melt migration controls on the trace element budget of the lower oceanic crust: Insights from the troctolite–olivone gabbro association of the Pineto ophiolite (Corsica, France). *Ofioliti*, *44*(2), 71–82. https://doi.org/10.4454/ofioliti.v44i2.525

Botazzi, P., Tiepolo, M., Vannucci, R., Zanetti, A., Brumm, R., Foley, S. F., & Oberti, R. (1999). Distinct site preferences for heavy and light REE in amphibole and the prediction of $^{Amph/L}D_{REE}$. *Contributions to Mineralogy and Petrology*, *137*, 36–45. https://doi.org/10.1007/s004100050580

Brueckner, H. K. (1998). Sinking intrusion model for the emplacement of garnet-bearing peridotites into continent collision orogens. *Geology*, *26*, 631–634. https://doi.org/10.1130/0091-7613(1998)026<0631:SIMFTE>2.3.CO;2

Burgess, S. R., & Harte, B. (2004). Tracing lithosphere evolution through the analysis of hererogeneou G9–G10 garnets in peridotite xenoliths, II. REE chemistry. *Journal of Petrology*, *45*, 609–634. https://doi.org/10.1093/petrology/egg095

Coleman, R. G. (1967). Alpine ultramafic rocks of California, Oregon and Washington. *Geological Survey Bulletin*, *1247*, 1–49.

Coogan, L. A., Gillis, K. M., MacLeod, C. J., Thompson, G. M., & Hékinian, R. (2002). Petrology and geochemistry of the lower ocean crust formed at the Pacific Rise and exposed at Hess Deep: A synthesis and new results. *Geochemistry, Geophysics, Geosystems*, *11*, 1–30. https://doi.org/10.1029/2001GC000230

Deschamps, F., Godard, M., Guillot, S., & Hattori, K. (2013). Geochemistry of subduction zone serpentinites: A review. *Lithos*, *178*, 96–127. https://doi.org/10.1016/j.lithos.2013.05.019

Duan, W.-Y., Li, X.-P., Schertl, H.-P., Willner, A. P., Wang, S.-J., Chen, S., & Sun, G.-M. (2021). Rodingitization records from ocean-floor to high pressure metamorphism in the Xigaze ophiolite, southern Tibet. *Gondwana Research*, *104*, 126–153. https://doi.org/10.1016/j.gr.2021.05.013

Dungan, M. A. (1979). Bastite pseudomorphs after orthopyroxene, clinopyroxene and tremolite. *Canadian Mineralogist*, *17*, 729–740.

Evans, B. W. (1977). Metamorphism of Alpine peridotite and serpentinite. *Annual Reviews in Earth and Planetary Sciences*, *5*, 397–447.

Evans, B. W., Hattori, K., & Baronnet, A. (2013). Serpentinite: What, Why, Where? *Elements*, *9*, 99–106.

Evans, B. W., & Trommsdorff, V. (1978). Petrogenesis of garnet lherzolite, Cima diGagnone, Lepontine Alps. *Earth and Planetary Science Letters*, *40*, 333–348.

Evans, B. W., Trommsdorff, V., & Richter, W. (1979). Petrology of an eclogite–metarodingite suite at Cima di Gagnone, Ticino, Switzerland. *American Mineralogist*, *64*, 15–31.

Evans, K. A., & Frost, B. R. (2021). Deserpentinization in subduction zones as a source of oxidation in arcs: A reality check. *Journal of Petrology*, *62*, 1–32. https://doi.org/10.1093/petrology/egab016

Frost, B. R., & Beard, J. S. (2007). On silica activity and serpentinization. *Journal of Petrology*, *48*, 1351–1368. https://doi.org/10.1093/petrology/egm021

Frost, B. R., Beard, J. S., McCaig, A., & Condliffe, E. (2008). The formation of micro-rodingites from IODP Hole U1309D: Key to understanding the process of serpentinization. *Journal of Petrology*, *49*, 1579–1588. https://doi.org/10.1093/petrology/egn038

Gillis, K. M., Ludden, J. N., & Smith, A. D. (1992). Mobilization of REE during crustal aging in the Troodos Ophiolite, Cyprus. *Chemical Geology*, *98*, 71–86. https://doi.org/10.1016/0009-2541(92)90091-I

Gose, J., & Schmädicke, E. (2018). Water incorporation in garnet: Coesite versus quartz eclogite from Erzgebirge and Fichtelgebirge. *Journal of Petrology*, *59*, 207–232. https://doi.org/10.1093/petrology/egy022

Grant, J. A. (2005). Isocon analysis: A brief review of the method and applications. *Physics and Chemistry of the Earth*, *30*, 997–1004. https://doi.org/10.1016/j.pce.2004.11.003

Gresens, R. L. (1967). Composition–volume relationships of metasomatism. *Chemical Geology*, *2*, 47–55. https://doi.org/10.1016/0009-2541(67)90004-6

Gussone, N., Austrheim, H., Westhues, A., & Mezger, K. (2020). Origin of rodingite forming fluids constrained by calcium and strontium isotope ratios in the Leka Ophiolite Complex. *Chemical Geology*, *542*, 119598. https://doi.org/10.1016/j.chemgeo.2020.119598

Hattori, K. H., & Guillot, S. (2003). Volcanic fronts form as a consequence of serpentinite dehydration in the forearc mantle wedge. *Geology*, *31*(6), 525–528. https://doi.org/10.1130/0091-7613(2003)031<0525:VFFAAC>2.0.CO;2

Honnorez, J., & Kirst, P. (1975). Petrology of rodingites from the equatorial Mid-Atlantic fracture zones and their geotectonic significance. *Contributions to Mineralogy and Petrology*, *49*, 233–257. https://doi.org/10.1007/BF00376590

Iyer, K., Austrheim, H., John, T., & Jamtveit, B. (2008). Serpentinization of the oceanic lithosphere and some geochemical consequences: Constraints from the Leka Ophiolite Complex, Norway. *Chemical Geology*, *249*, 66–90. https://doi.org/10.1016/j.chemgeo.2007.12.005

Klemd, R., & Schmädicke, E. (1994). High-pressure metamorphism in the Münchberg Gneiss Complex and the Erzgebirge Crystalline Complex: The roles of fluid and reaction kinetics. *Geochemistry – Chemie der Erde*, *54*, 241–261.

Koglin, N., Zeh, A., Franz, G., Schüssler, U., Glodny, J., Gerdes, A., & Brätz, H. (2018). From Cadomian magmatic arc to Rheic ocean closure: The geochronological–geochemical record of nappe protoliths of the Münchberg Massid, NE Bavaria (Germany). *Gondwana Research*, *55*, 135–152. https://doi.org/10.1016/j.gr.2017.11.001

Koller, F., & Richter, W. (1984). Die Metarodingite der Habachformation, Hohe Tauern (Österreich). *Tschermaks Mineralogische und Petrographische Mitteilungen*, *33*, 49–66. https://doi.org/10.1007/BF01082301

Koutsovitis, P., Magganas, A., Pomonos, P., & Ntaflos, T. (2013). Subduction-related rodingites from East Othris, Greece: Mineral reactions and physicochemical conditions of formation. *Lithos*, *172–173*, 139–157. https://doi.org/10.1016/j.lithos.2013.04.009

Laborda-López, C., López-Sánchez-Vizcaíno, V., Marchesi, C., Gómez-Pugnaire, M. T., Garrido, C. J., Jabaloy-Sánchez, A., Padrón-Navarta, J. A., & Hidas, K. (2018). High-*P* metamorphism of rodingites during serpentinite dehydration (Cerro del Almirez, Southern Spain): Implications for the redox state in subduction zones. *Journal of Metamorphic Geology*, *36*, 1141–1173. https://doi.org/10.1111/jmg.12440

Li, X.-P., Rahn, M., & Bucher, K. (2008). Eclogite facies metarodingites–phase relations in the system SiO_2–Al_2O_3–Fe_2O_3–FeO–MgO–CaO–CO_2–H_2O: An example from the Zermatt-Saas ophiolite. *Journal of Metamorphic Geology*, *26*, 347–364. https://doi.org/10.1111/j.1525-1314.2008.00761.x

Li, X.-P., Zhang, L., Wie, C., Ai, Y., & Chen, J. (2007). Petrology of rodingite derived from eclogite in western Tienshan, China. *Journal of Metamorphic Geology*, *25*, 363–382. https://doi.org/10.1111/j.1525-1314.2007.00700.x

Liou, J. G., Zhang, R. Y., & Ernst, W. G. (2007). Very high-pressure orogenic garnet peridotite. *Proceedings of the National Academy of Sciences*, *104*, 9116–9121. https://doi.org/10.1073/pnas.0607300104

Liou, J. G., Zhang, R. Y., Ernst, W. G., Rumble, D., & Maruyama, S. (1998). High-pressure minerals from deeply subducted metamorphic rocks. *Reviews in Mineralogy*, *37*, 33–96. https://doi.org/10.1515/9781501509179-004

Marcaillou, C., Munoz, M., Vidal, O., Parra, T., & Harfouche, M. (2011). Mineralogical evidence for H_2 degassing during serpentinization at 300 °C/33 bar. *Earth and Planetary Science Letters*, *303*, 281–290. https://doi.org/10.1016/j.epsl.2011.01.006

Massonne, H.-J. (2001). First find of coesite in the ultrahigh-pressure metamorphic region of the Central Erzgebirge, Germany. *European Journal of Mineralogy*, *13*, 565–570. https://doi.org/10.1127/0935-1221/2001/0013-0565

Massonne, H.-J., & Czambor, A. (2007). Geochemical signatures of Variscan eclogites from the Saxonian Erzgebirge, central Europe. *Geochemistry – Chemie der Erde*, *67*, 69–83. https://doi.org/10.1016/j.chemer.2006.07.001

Mathé, G. (1990). Zur Geologie der Serpentinitvorkommen im sächsischen Erzgebirge. *Abhandlungen des Staatlichen Museums für Mineralogie und Geologie Dresden*, *37*, 55–72.

McDonough, W. F., & Sun, S. S. (1995). The composition of the Earth. *Chemical Geology*, *120*, 223–253. https://doi.org/10.1016/0009-2541(94)00140-4

Mével, C. (2003). Serpentinization of abyssal peridotites at mid-ocean ridges. *Comptes Rendus Geoscience*, *335*, 825–852. https://doi.org/10.1016/j.crte.2003.08.006

Miyashiro, A., Shido, F., & Ewing, M. (1969). Composition and origin of serpentinites from the Mid-Atlantic Ridge near 24 and 30°N. *Contributions to Mineralogy and Petrology*, *23*, 117–127. https://doi.org/10.1007/BF00375173

Nasdala, L., & Massonne, H.-J. (2000). Microdiamonds from the Saxonian Erzgebirge, Germany: In situ micro-Raman characterization. *European Journal of Mineralogy*, *12*, 495–498. https://doi.org/10.1127/0935-1221/2000/0012-0495

O'Hanley, D. S., Schandl, E. S., & Wicks, F. J. (1992). The origin of rodingites from Cassiar, British Columbia, and their use to estimate T and P(H_2O) during serpentinization. *Geochimica et Cosmochimica Acta*, *56*, 97–108. https://doi.org/10.1016/0016-7037(92)90119-4

Palandri, J. L., & Reed, M. H. (2004). Geochemical models of metasomatism in ultramafic systems: Serpentinization, rodingitization, and sea floor carbonate chimney precipitation. *Geochimica et Cosmochimica Acta*, *68*, 1115–1133. https://doi.org/10.1016/j.gca.2003.08.006

Pearce, N. J. G., Perkins, W. T., Westgate, J. A., Gorton, M. P., Jackson, S. E., Neal, C. R., & Chenery, S. P. (1997). A compilation of new and published major and trace element data for NIST SRM 610 and NIST SRM 612 glass reference materials. *Geostandards Newsletter*, *21*, 115–144. https://doi.org/10.1111/j.1751-908X.1997.tb00538.x

Pettke, T., & Bretscher, A. (2022). Fluid-mediated element cycling in subducted oceanic lithosphere: The orogenic serpentinite perspective. *Earth-Science Reviews*, *225*, 103896.

Ranero, C. R., Morgan, J. P., McIntosh, K., & Reichert, C. (2003). Bending-related faulting and mantle serpentinization at the Middle America trench. *Nature*, *425*, 367–373. https://doi.org/10.1038/nature01961

Rötzler, K., Schumacher, R., Maresch, W. V., & Willner, A. P. (1998). Characterization and geodynamic implications of contrasting metamorphic evolution in juxtaposed high-pressure units of the Western Erzgebirge (Saxony, Germany). *European Journal of Mineralogy*, *10*, 261–280. https://doi.org/10.1127/ejm/10/2/0261

Sächsisches Landesamt für Umwelt, Landwirtschaft und Geologie, Freistaat Sachsen. (2020). Geologische Karten des Freistaats Sachsen 1:25,000.

Salvioli-Mariani, E., Boschetti, T., Toscani, L., Montanini, A., Petriglieri, J. A., & Bersani, D. (2020). Multi-stage rodingitization of ophiolitic bodies from Northern Apennines (Italy): Constraints from petrography, geochemistry and thermodynamic modelling. *Geoscience Frontiers*, *11*, 2103–2125. https://doi.org/10.1016/j.gsf.2020.04.017

Schandl, E. S., O'Hanley, D. S., & Wicks, F. J. (1989). Rodingites in serpentinized ultramafic rocks of the Abatiti Greenstone Belt, Ontario. *Canadian Mineralogist*, *27*, 579–591.

Schmädicke, E. (1991). Quartz pseudomorphs after coesite in eclogites from the Saxonian Erzgebirge. *European Journal of Mineralogy*, *3*, 231–238. https://doi.org/10.1127/ejm/3/2/0231

Schmädicke, E. (1994). *Die Eklogite des Erzgebirges Freiberger Forschungsheft* (Vol. C 456) (p. 338). Deutscher Verlag für Grundstoffindustrie.

Schmädicke, E., & Evans, B. W. (1997). Garnet-bearing ultramafic rocks from the Erzgebirge, and their relation to other settings in the Bohemian Massif. *Contributions to Mineralogy and Petrology*, *127*, 57–74. https://doi.org/10.1007/s004100050265

Schmädicke, E., & Gose, J. (2017). Water transport by subduction: Clues from garnet of Erzgebirge UHP eclogite. *American Mineralogist*, *102*, 975–986. https://doi.org/10.2138/am-2017-5920

Schmädicke, E., & Gose, J. (2019). Low water contents in garnet of orogenic peridotite: Clues for an abyssal or mantle-wedge origin? *European Journal of Mineralogy*, *31*(4), 715–730. https://doi.org/10.1127/ejm/2019/0031-2880

Schmädicke, E., & Gose, J. (2020). Water in garnet of garnetite (metarodingite) and eclogite from the Erzgebirge and the Lepontine Alps. *Journal of Metamorphic Geology*, *38*, 905–933. https://doi.org/10.1111/jmg.12554

Schmädicke, E., Gose, J., Reinhardt, J., Will, T. M., & Stalder, R. (2015). Garnet in cratonic and non-cratonic mantle and lower crustal xenoliths from southern Africa: Composition, water incorporation and geodynamic constraints. *Precambrian Research*, *270*, 285–299. https://doi.org/10.1016/j.precamres.2015.09.019

Schmädicke, E., Gose, J., & Will, T. (2010). The *P–T* evolution of ultra high temperature garnet-bearing ultramafic rocks from the Saxonian Granulitgebirge Core Complex, Bohemian Massif. *Journal of Metamorphic Geology*, *28*, 489–508. https://doi.org/10.1111/j.1525-1314.2010.00876.x

Schmädicke, E., Mezger, K., Cosca, M. A., & Okrusch, M. (1995). Variscan Sm–Nd and Ar–Ar ages of eclogite-facies rocks from the Erzgebirge, Bohemian Massif. *Journal of Metamorphic Geology*, *13*, 537–552. https://doi.org/10.1111/j.1525-1314.1995.tb00241.x

Schmädicke, E., Okrusch, M., & Schmidt, W. (1992). Eclogite-facies rocks in the Saxonian Erzgebirge, Germany: High pressure metamorphism under contrasting *P–T* conditions. *Contributions to Mineralogy and Petrology*, *110*, 226–241. https://doi.org/10.1007/BF00310740

Schmädicke, E., & Will, T. (2021). No chemical change during high-T dehydration and re-hydration reactions: Constraints from Erzgebirge HP and UHP eclogite. *Lithos*, *386–387*, 105995. https://doi.org/10.1016/j.lithos.2021.105995

Schmädicke, E., Will, T., & Mezger, K. (2015). Garnet pyroxenite from the Shackleton Range, Antarctica: Intrusion of plume-derived picritic melts in the continental lithosphere during Rodinia breakup? *Lithos*, *238*, 185–206. https://doi.org/10.1016/j.lithos.2015.09.016

Schmädicke, E., Will, T. M., Ling, X., Li, X.-H., & Li, Q. (2018). Rare peak and ubiquitous post-peak zircon in eclogite: Constraints for the timing of UHP and HP metamorphism in Erzgebirge, Germany. *Lithos*, *322*, 250–267. https://doi.org/10.1016/j.lithos.2018.10.017

Schwarzenbach, E. M., Caddick, M. J., Petroff, M., Gill, B. C., Cooperdock, E. H. G., & Barnes, J. D. (2018). Sulphur and carbon cycling in the subduction zone mélange. *Scientific Reports*, *8*, 15517. https://doi.org/10.1038/s41598-018-33610-9

Seyler, M., Cannat, M., & Mével, C. (2003). Evidence for major-element heterogeneity in the mantle source of abyssal peridotites from the Southwest Indian Ridge (52° to 68°E). *Geochemistry, Geophysics, Geosystems*, *4*(2), 9101. https://doi.org/10.1029/2002GC000305

Smith, D., & Griffin, W. L. (2005). Garnetite xenoliths and mantle–water interactions below the Colorado plateau, southwestern United States. *Journal of Petrology*, *46*, 1901–1924. https://doi.org/10.1093/petrology/egi042

Stachel, T., Aulbach, S., Brey, G. P., Harris, J. W., Leost, I., Tappert, R., & Viljoen, K. S. (2004). The trace element composition of silicate inclusions in diamonds: A review. *Lithos*, *77*, 1–19. https://doi.org/10.1016/j.lithos.2004.03.027

Stöckhert, B., Duyster, J., Trepmann, C., & Massonne, H. J. (2001). Microdiamond daughter crystals precipitated from supercritical COH silicate fluids included in garnet, Erzgebirge, Germany. *Geology*, *29*, 391–394. https://doi.org/10.1130/0091-7613(2001)029<0391:MDCPFS>2.0.CO;2

Stosch, H. G., & Lugmair, G. W. (1990). Geochemistry and evolution of MORB-type eclogites from the Münchberg Massif, southern Germany. *Earth and Planetary Science Letters*, *99*, 230–249. https://doi.org/10.1016/0012-821X(90)90113-C

Tenthorey, E., & Hermann, J. (1979). Composition of fluids during serpentinite breakdown in subduction zones: Evidence for limited boron mobility. *Geology*, *32*, 865–868.

Tichomirowa, M., Berger, H.-J., Koch, E. A., Belyatski, B. V., Götze, J., Kempe, U., & Schaltegger, U. (2001). Zircon ages of high-grade gneisses in the Eastern Erzgebirge (Central European Variscides)—Constraints on origin of the rocks and Precambrian to Ordovician magmatic events in the Variscan foldbelt. *Lithos*, *56*, 303–332. https://doi.org/10.1016/S0024-4937(00)00066-9

Tichomirowa, M., & Köhler, R. (2013). Discrimination of protolithic versus metamorphic zircon ages in eclogites: Constraints from the Erzgebirge metamorphic core complex (Germany). *Lithos*, *177*, 436–450. https://doi.org/10.1016/j.lithos.2013.07.013

Timmermann, H., Štědrá, V., Gerdes, A., Noble, S. R., Parrish, R. R., & Dörr, W. (2004). The problem of dating high-pressure metamorphism: A U–Pb isotope and geochemical study on eclogites and related rocks of the Mariánské Lázně Complex, Czech Republic. *Journal of Petrology*, *45*, 1311–1338. https://doi.org/10.1093/petrology/egh020

Van Achterbergh, E., Ryan, C. G., & Griffin, W. L. (2000). *GLITTER: On-line interactive data reduction for the laser ablation ICPMS microprobe*. Macquarie University.

Will, T. M., Lee, S.-H., Schmädicke, E., Frimmel, H. E., & Okrusch, M. (2015). Variscan terrane boundaries in the Odenwald–Spessart basement, Mid-German Crystalline Zone: New evidence from ocean ridge, intraplate and arc-derived metabasaltic rocks. *Lithos*, *220–223*, 23–42. https://doi.org/10.1016/j.lithos.2015.01.018

Will, T. M., & Schmädicke, E. (2001). A first report of retrogressed eclogites in the Odenwald Crystalline Complex: Evidence for high-pressure metamorphism in the Mid-German Crystalline Rise, Germany. *Lithos*, *59*, 109–125. https://doi.org/10.1016/S0024-4937(01)00059-7

Winchester, J. A., & Floyd, P. A. (1977). Geochemical discrimination of different magmaseries and their differentiation products using immobile elements. *Chemical Geology*, *20*, 325–343.

Woodland, A. B., Seitz, H.-M., Altherr, R., Marschall, H., Olker, B., & Ludwig, T. (2002). Li abundances in eclogite minerals: A clue to a crustal or mantle origin? *Contributions to Mineralogy and Petrology*, *143*, 587–601. https://doi.org/10.1007/s00410-002-0363-8

SUPPORTING INFORMATION

Additional supporting information can be found online in the Supporting Information section at the end of this article.

Table S1: Major element composition (wt.%) of rodingite or metarodingite (rock names as given in literature) and garnetite (interpreted as meta-rodingite) with relatively low CaO contents that formed by metasomatism of mafic protoliths during serpentinization of adjacent ultramafic rocks.
Table S2: Absolute and relative (%) standard deviation (STD) of ICP analyses.
Table S3: Analysis of secondary standard BE-N showing the measured average (Avg), standard deviation (STD) and accuracy (Acc).
Table S4: Selected Microprobe analyses of garnet (grt) from garnetite (Gra) and eclogite (Ecl). Oxides in wt.%; formula normalized to 12 oxygen atoms.
Table S5: Selected Microprobe analyses of clinopyroxene (cpx) from garnetite (Gra) and eclogite (Ecl). Oxides in wt.%; formula normalized to 6 oxygen atoms.
Appendix S1: Cumulate origin of garnetite protolith?
Table S6: Inferred mineral compositions for the igneous protolith deduced from the average bulk rock analysis of garnetite. Cations were normalized to 4 (olivine), 8 (plagioclase), and 6 (clinopyroxene) oxygens.
Table S7: Calculated bulk compositions of olivine–plagioclase and olivine–plagioclase–clinopyroxene mixtures using the mineral compositions in Table S3 compared to the actual bulk rock composition of garnetite. The composition of any theoretical mixture does not match that of Erzgebirge garnetite. Elements or element ratios with the greatest mismatch are shown in red.
Table S8: Data compilation for abyssal peridotite from the Mid-Atlantic Ridge, ODP-Leg 153, comparing CaO content and degree of serpentinization*.
Figure S1: Plot of CaO content versus degree of serpentinization of abyssal peridotite from the Mid-Atlantic Ridge, ODP-Leg 153. Data from Table S8.
Appendix S2: References Supporting Information.

How to cite this article: Schmädicke, E., & Will, T. M. (2023). Origin of Erzgebirge ultrahigh-pressure garnetite: Formation from a basaltic protolith by serpentinization-assisted metasomatism? *Journal of Metamorphic Geology*, *41*(9), 1237–1259. https://doi.org/10.1111/jmg.12742